

# Concentrations of dissolved dimethyl sulphide (DMS), methanethiol and other trace gases in context of microbial communities from the temperate Atlantic to the Arctic Ocean

Valérie Gros<sup>1</sup>, Bernard Bonsang<sup>1</sup>, Roland Sarda-Estève<sup>1</sup>, Anna Nikolopoulos<sup>2</sup>, Katja Metfies<sup>3</sup>, Matthias  
5 Wietz<sup>3,4</sup> and Ilka Peeken<sup>3</sup>

<sup>1</sup> Laboratoire des Sciences du Climat et de l'Environnement, CNRS-CEA-UVSQ, IPSL, Gif sur Yvette, 91 191, France

<sup>2</sup> Norwegian Polar Institute, Fram Centre, 9296 Tromsø, Norway

<sup>3</sup> Alfred Wegener Institute Helmholtz Centre for Polar and Marine Research, 27570 Bremerhaven, Germany

<sup>4</sup> Max Planck Institute for Marine Microbiology, 28359 Bremen, Germany

10

Correspondence to: Valérie Gros ([valerie.gros@lsce.ipsl.fr](mailto:valerie.gros@lsce.ipsl.fr))

## Abstract.

Dimethyl sulphide (DMS) plays an important role in the atmosphere by influencing the formation of aerosols and cloud  
15 condensation nuclei. In contrast, the role of methanethiol (MeSH) for the budget and flux of reduced sulphur remains poorly  
understood. In the present study, we quantified DMS and MeSH together with the trace gases carbon monoxide (CO), isoprene,  
acetone, acetaldehyde and acetonitrile in North Atlantic and Arctic Ocean surface waters, covering a transect from 57.2°N to  
80.9°N in high spatial resolution in May-June 2015. Whereas isoprene, acetone, acetaldehyde and acetonitrile concentrations  
decreased northwards, CO, DMS and MeSH retained substantial concentrations at high latitudes, indicating specific sources  
20 in polar waters. DMS was the only compound with higher average in polar ( $31.2 \pm 9.3$  nM) than in Atlantic waters ( $13.5 \pm 2$   
nM), presumably due to DMS originating from sea ice. At eight sea-ice stations north of 80°N, in the diatom-dominated  
marginal ice zone, DMS and chlorophyll a markedly correlated ( $R^2 = 0.93$ ) between 0-50 m depth . In contrast to previous  
studies, MeSH and DMS did not co-vary, indicating decoupled processes of production and conversion. The contribution of  
MeSH to the sulphur budget (represented by DMS+MeSH) was on average 20% (and up to 50%) higher than previously  
25 observed in the Atlantic and Pacific Oceans, suggesting MeSH as an important source of sulphur possibly emitted to the  
atmosphere. The potential importance of MeSH was underlined by several correlations with bacterial taxa, including typical  
phytoplankton associates from the *Rhodobacteraceae* and *Flavobacteriaceae* families. Furthermore, the correlation of isoprene  
and chlorophyll a with *Alcanivorax* indicated a specific relationship with isoprene-producing phytoplankton. Overall, the  
demonstrated latitudinal and vertical patterns contribute to understanding how concentrations of central marine trace gases are  
30 linked with chemical and biological dynamics across oceanic waters.

## 1 Introduction

35 Volatile Organic Compounds (VOCs) and carbon monoxide (CO) are important in atmospheric chemistry as precursors of ozone and secondary organic aerosols, which affect air quality and climate. Despite being a relatively small source compared to anthropogenic emissions (Duncan et al., 2007; Kansal, 2009) and terrestrial vegetation (Guenther et al., 1995), the global oceans are increasingly considered as sources and sinks of CO and VOCs with potential influence on atmospheric chemistry, Biological activity substantially contribute to the dynamics of short-lived VOCs like dimethyl sulphide (DMS) and isoprene. For instance, dimethylsulfoniopropionate (DMSP) produced by phytoplankton and other marine organisms (such as macroalgae, corals and sponges, Jackson and Gabric, 2022 and references therein) can be metabolized by bacteria into DMS. DMS 40 is rapidly oxidized once emitted to the atmosphere (1 day mean lifetime, Kloster et al., 2006), then representing a major precursor of sulphated aerosols with radiative impacts by scattering sunlight and constituting condensation nuclei (CCN), potentially cooling the climate through changing cloud microphysics. The role of DMS emissions on climate was first hypothesized by Shaw, (1983) and Charlson et al., (1987) and is known as the CLAW hypothesis, which has been largely discussed and debated since then. There is extensive literature on both the link between DMSP and DMS as well as on the 45 multi-steps of the oxidation of DMS to sulphate and the corresponding impact on CCN. As both processes are beyond the scope of this paper, we refer the reader to the recent review of Jackson and Gabric (2022) and references therein for further information. Alternatively, DMSP can be microbially demethylated into methanethiol ( $\text{CH}_3\text{SH}$ , here referred to as MeSH) (Kiene, 1996; Kiene and Linn, 2000), whose role in the atmosphere and oceans is poorly characterized to date (Lawson et al., 2020). The oxidation of MeSH by hydroxyl radicals (Tyndall and Ravishankara, 1991; Butkovskaya and Setser, 1999) is 50 estimated to effectively produce  $\text{SO}_2$  with up to 48% based on model calculations (Novak et al., 2022). Thus, MeSH is probably an underestimated factor in the marine sulphur cycle.

Isoprene, another important trace gas, can be produced by photosynthesizing organisms over short timescales (a few hours), with potential influence on regional atmospheric chemistry and aerosol formation above biologically active pelagic waters (Bikkina et al., 2014). Photosynthetic cyanobacteria are stronger emitters of isoprene than diatoms, with taxon-specific 55 variability in production (Bonsang et al., 2010; Shaw et al., 2010). Besides direct emission by primary producers, oceanic trace gases can originate from photochemical processes. For instance, isoprene can also be photochemically produced at the sea-surface microlayer (Ciuraru et al., 2015). In addition, photodegradation of dissolved organic matter is the main source of CO (Wilson et al., 1970), although laboratory experiments showed a minor contribution of biological activities (Gros et al., 2009).

The oceanic contribution to the budget of oxygenated VOCs (OVOC) like acetone, acetaldehyde and methanol is also 60 important to consider, since OVOCs may affect the oxidative capacity of the remote atmosphere through tropospheric radicals (Singh, 2004). A recent study has confirmed the importance of air-sea exchange for acetaldehyde, pointing out the lack of oceanic measurements (Wang et al., 2019). Marine waters can be either a local source or sink of OVOCs depending on the region. Acetone and acetaldehyde are considered to originate from photodegradation of dissolved organic carbon (Zhou and

Mopper, 1997; Zhu and Kieber, 2019). A positive net flux of acetone is generally observed in biologically productive areas such as tropical upwelling zones, whereas high-latitude and oligotrophic waters represent sinks (Lawson et al., 2020). As OVOCs mainly originate from terrestrial sources, their air-sea fluxes can also be a net deposition, when their marine atmospheric concentrations are directly influenced by air masses originating from continents (Phillips et al., 2021). Furthermore, OVOCs can show seasonal variation (Davie-Martin et al., 2020).

Linking the dynamics of (O)VOCs and trace gases to primary production and microbial distribution helps to understand fundamental couplings between biological, oceanic and atmospheric processes. This is particularly important in the Arctic Ocean, which currently is observed to warm two to three times faster than the global average (Schmale et al., 2021 and references therein). These processes concur with changing physical, biological and photochemical variability, subsequently affecting the coupling between ocean and atmosphere. Importantly, sea-ice melt influences VOCs production, e.g. through increased primary production in ice-free waters (Arrigo and van Dijken, 2015), release of ice algae and their substrates (Fernández-Méndez et al., 2014), as well as higher gas exchange at the ocean-atmosphere interface (Lannuzel et al., 2020) when ice-free areas expand. This influence of sea-ice has been shown for DMSP, DMS, isoprene, acetone and acetaldehyde in the Canadian Arctic (Galindo et al., 2014; Wohl et al., 2022; Galí et al., 2021). Concurrent changes in phytoplankton distribution can amplify these dynamics, for instance via the northward expansion of the coccolithophorid *Emiliania huxleyi* by Atlantic currents (Hegseth and Sundfjord, 2008; Oziel et al., 2020) and changing bloom phenologies (Nöthig et al., 2015; von Appen et al., 2021). As phytoplankton and bacterial distribution are often linked, these dynamics subsequently affect the heterotrophic food web. The bacterial families *Rhodobacteraceae* and *Flavobacteriaceae* are frequently abundant during phytoplankton blooms, contributing to the degradation of algal organic matter and the conversion of DMSP into DMS and MeSH (Moran et al., 2012; Moran and Durham, 2019). Campen et al., (2022) have recently emphasized the need to better link bacterial distribution with DMS and CO metabolism. In addition, the production and degradation of isoprene could be an important, yet understudied contribution to biogeochemical cycles (Carrión et al., 2020; Rodríguez-Ros et al., 2020; Simó et al., 2022).

As Atlantic characteristics are observed to expand northward with climate change (Polyakov et al., 2020), it is important to contextualize marine VOCs, trace gases and microbes in Arctic versus temperate Atlantic waters. Here, we report concentrations of DMS, MeSH, isoprene, CO, acetone, acetaldehyde and acetonitrile in context of microbial distribution across the North Atlantic and Arctic Oceans. During the TRANSSIZ campaign onboard RV Polarstern from early spring to summer 2015, we continuously measured these compounds in surface waters between 57° to 80°N, and additionally over vertical profiles from the surface to 50 m depth in the ice-covered region north of Svalbard (Fig. 1). The main objective was to document the concentrations and spatial variability of trace gases, specifically the ratio between MeSH and DMS, in context of phytoplankton biomass, bacterial diversity and water masses. To our knowledge, this is the first survey of MeSH in the Arctic Ocean, shedding light on its biogeochemical role in an area of rapid climate change.

## 2 Material and methods

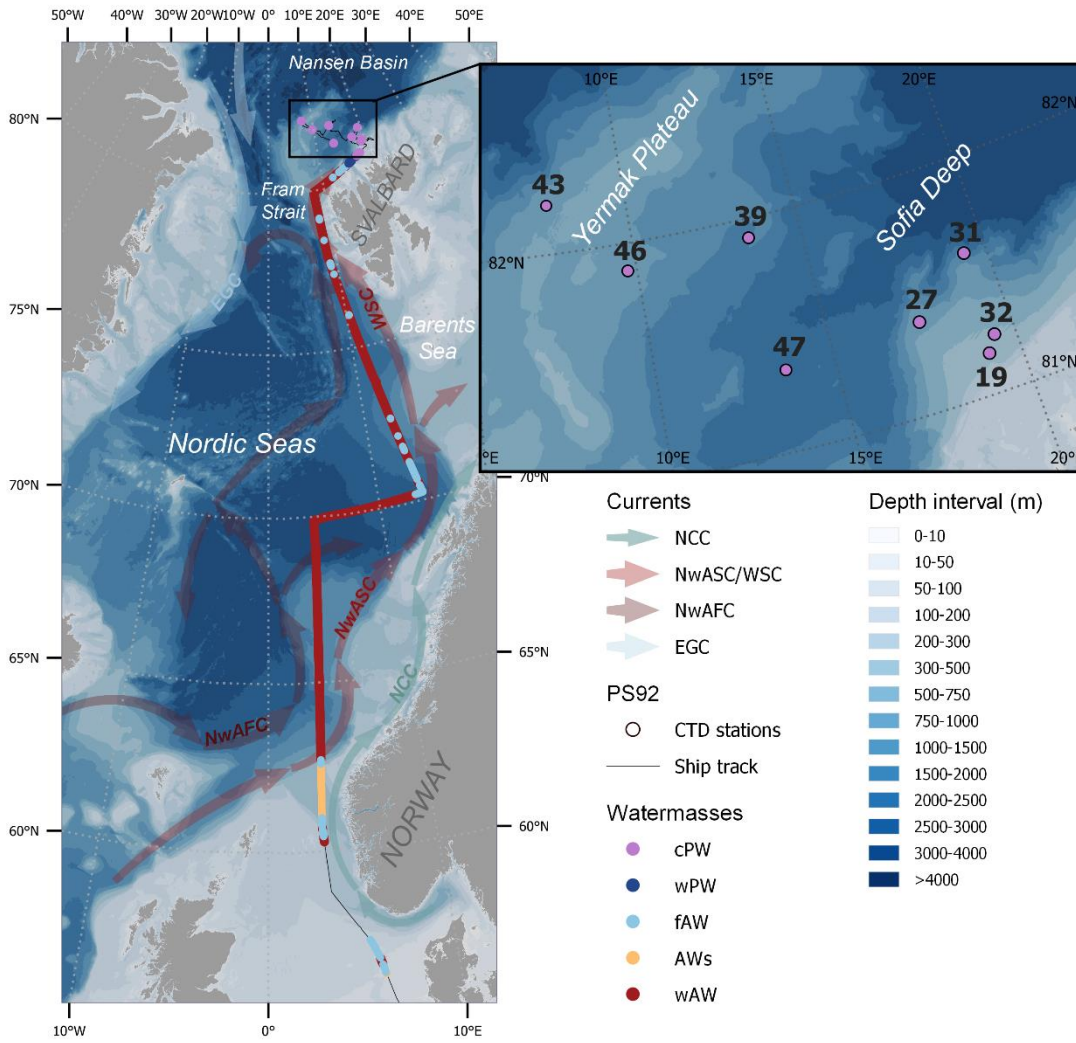
### 2.1 Campaign description and oceanographic parameters

100 Water samples were collected during the TRANSIZ (“Transitions in the Arctic Seasonal Sea Ice Zone”; PS 92 - ARK XXIX/1) cruise onboard RV Polarstern between May 19<sup>th</sup> and June 28<sup>th</sup>, 2015. The cruise started in Bremerhaven, Germany, and ended in Longyearbyen, Svalbard (Fig. 1), as described in detail by Peeken (2016).

105 Along the ship track between May 19<sup>th</sup> and 27<sup>th</sup>, temperature, salinity and chlorophyll a (Chl a) fluorescence in the surface water layer (6 m depth) were continuously recorded with the FerryBox System of the Helmholtz-Zentrum Geesthacht, and extracted from the FerryBox database every 2 minutes. The instrument performs a self-cleaning routine every day, including acid washing and freshwater rinsing. In addition, sensor behavior is controlled by staff members of Polarstern, although drift of the sensors is very rarely observed (for details see Petersen (2014)). The sensor for Chl a was a submersible fluorometer (Turner Designs, Sunnyvale, CA, USA) with excitation/emission wavelengths of 460 nm and 620-715 nm respectively.

110 After May 27<sup>th</sup>, eight ice stations (number 19, 27, 31, 32, 39, 43, 46, and 47, Table S1) were carried out over the continental shelf north of Svalbard and over the Yermak Plateau (Fig. 1; Table S1). At each ice station, the ship was anchored to an ice floe at drift for approximately 36 h. While carrying out ice work on the port side, winch-operated instruments were deployed in the open water on the starboard side to record biological and biogeochemical variables including trace gases and phytoplankton pigments. Except for the first ice station (70% ice cover and still some leads present), the stations were conducted in almost 100% ice cover (Massicotte et al., 2019) with the sampling taking place in small leads. All ice stations were 50 to 250 km away from the ice edge and open water (Dybwad et al., 2021). A detailed study of nutrients, marker pigments and protist microscopy classified the Yermak Plateau stations (39, 43, 46) to be in a pre-bloom phase, while all other stations were in a bloom phase (Dybwad et al., 2021). During the ice stations, discrete seawater samples for trace gas and phytoplankton analyses were collected at six water depths between 0.5 and 50 m depth using 12 L Niskin bottles on the ship-CTD (conductivity, temperature, depth) water-sampling carousel. For trace gases, these samples were transferred to 1 L light-proof glass flasks for direct analysis on board. Values for temperature and salinity were provided by the CTD bottle data file for each station (Nikolopoulos et al., 2016).

120 Temperature and salinity from both types of measurements were used to classify the sampled water masses based on the criteria applied in Tran et al., 2013 (Table1).



125 Fig. 1: Ship track colored by water mass: ‘regular’ warm Atlantic Water (wAW), coastal-influenced Atlantic water with low salinity (AWs),  
 130 freshened and cooled Atlantic Water (fAW), warm Polar Water (wPW) and cold Polar Water (wPW), determined according to the  
 temperature and salinity criteria in Table 1. Surface measurements were done continuously between 57°N and 81°N, while vertical profiles  
 were sampled at eight sea ice stations (black insert and Table S1). The background map shows bathymetry (GEBCO, 2022) and a schematic  
 overview of the major currents influencing the surface waters in the study area, as adopted from Skagseth et al. (2022): the Norwegian  
 Atlantic Slope Current (NwASC), West Spitsbergen Current (WSC), Norwegian Atlantic Front Current (NwAFC), Norwegian Coastal  
 Current (NCC) and East Greenland Current (EGC).

## 2.2 Biological measurements

### 135 2.2.1 Pigment analysis

For pigment analysis with high pressure liquid chromatography (HPLC), seawater samples (1–2 L) were taken from the ship-CTD Niskin bottles from six depths in the upper 50 m (Table S1). All samples were processed within few hours after collection. Sample handling and pigment measurements were carried out as described in Tran et al. (2013). The FerryBox/surface Chl a data were calibrated against surface Chl a concentrations derived from the Niskin bottles ( $R^2 = 0.83$ , see Fig. S1). The taxonomic composition of phytoplankton was calculated from marker pigments using the CHEMTAX approach (for details see Wollenburg et al., (2018)), distinguishing diatoms, *Phaeocystis*-type haptophytes, prasinophytes, chlorophytes, dinoflagellates, cryptophytes, chrysophytes and coccolithophorid-type haptophytes. The contribution of each group was expressed as Chl a concentration.

### 2.2.2 Bacterial community analysis

145 A total of 34 seawater samples for bacterial community analysis were collected along the transect (Table S2) at a depth of ~10 m using the AUTOFIM system (Metfies et al., 2016, 2020), which is installed at the bow of the ship, next to the its pump system intake. Per sampling event, two L of seawater were filtered onto polycarbonate filters with 45 mm diameter and 0.4  $\mu\text{m}$  pore size (Millipore; USA) at 200 mbar. Filters were stored at  $-80^\circ\text{C}$  until DNA extraction in the home laboratory using the NucleoSpin Plant II kit (Macherey-Nagel, Germany) according to the manufacturer's instructions. Bacterial 16S rRNA gene fragments were amplified using primers 515F–926R (Parada et al., 2016) according to the 16S Metagenomic Sequencing Library Preparation protocol (Illumina, San Diego, CA). Amplicon gene libraries were sequenced using Illumina MiSeq technology in 2x300 bp paired-end runs at CeBiTec (Bielefeld, Germany). Raw sequence files have been deposited in the European Nucleotide Archive under accession number PRJEB50492, using the data brokerage service of the German Federation for Biological Data (GFBio) in compliance with MIxS standards. The complete amplicon analysis workflow is described in Supplement S2, with Rscripts documented under <https://github.com/matthiaswietz/transsiz>. Briefly, after primer removal using cutadapt (Martin, 2011), reads were classified into amplicon sequence variants (ASVs) using DADA2 (Callahan et al., 2016) and taxonomically classified using the Silva v138 database (Quast et al., 2012). We obtained on average 85,000 quality-controlled, chimera-filtered reads per sample (Table S2) sufficiently covering community composition (Fig. S2). Nonmetric multidimensional scaling was performed to determine bacterial community variability along the transect. Associations between the abundance of bacterial ASVs and environmental parameters were determined via Holm-corrected Spearman's correlations. Only correlations  $>|0.4|$  were considered, and only if higher than correlations with latitude to omit indirect signals due to geographical variability.

## 2.3 Trace gas measurements

165 Carbon monoxide and VOCs dissolved in seawater were measured in real-time along the transect using samples from the  
FerryBox water intake (6 m depth). Seawater was delivered by the ship membrane pump to the laboratory for continuous  
injection into an online water extraction device (OLWED; Supplement S3, Fig. S3). Furthermore, we measured trace gas  
concentrations from 0.5 to 50 m depth at the eight ice stations, analysing all samples within few hours after collection. Possible  
artifacts from storage have been investigated in a previous experiment in the same area (Tran et al., 2013), showing no  
170 significant losses of low molecular weight VOCs and a slow decrease for CO during the first 4 hours (Xie and Zafiriou, 2009  
and Tolli and Taylor, 2005). As no cross calibration was made between transect and Niskin measurements, possible differences  
between on-line and off-line measurements could not be evaluated.

### 2.3.1 PTRMS measurements

VOCs were quantified using a high-sensitivity Proton-Transfer Mass Spectrometer (PTRMS, Ionicon Analytik) developed by  
175 Lindinger and Jordan (1998) and since then widely used (reviewed by Blake et al., (2009)). The measurement principle of  
PTRMS is based on the soft chemical ionization of VOCs by proton transfer, which is possible for all compounds with a proton  
affinity higher than water, giving access to a variety of VOCs (Blake et al., 2009). During the campaign, air from the headspace  
was continuously sampled by the PTRMS through a 1/8 inch PFA line at a flowrate of about 60 ml/min using standard  
parameters, i.e. 60°C (inlet and drift tube temperature), 600V drift tube, and 2.2 mbar drift tube pressure (with a corresponding  
180 E/N of 132 Townsend). The estimated residence time of about 30 seconds should prevent degradation or adsorption of extracted  
gases in the system. Furthermore, a series of standards were measured under the same experimental conditions, showing high  
linearity in the system's response supporting the absence of artifacts. Measurements were typically performed every 2.5  
minutes, except between 61.1 °N to 65.3°N, where measurements were performed every 10 min for approximately 24 h, to  
scan a wider range of masses (m/z). This step was needed to select the compounds of interest, i.e. those showing a signal above  
185 the detection limit. About 25 masses (m/z) were selected to be further monitored (with dwell times from 1 to 20 s). Here, we  
present the results for the compounds with the most significant variability: isoprene (m/z 69), dimethyl sulphide (m/z 63),  
methanethiol (m/z 49), acetone (m/z 59), acetaldehyde (m/z 45), and acetonitrile (m/z 42). The only small fragmentation from  
soft ionization allows direct measurements of compounds at their corresponding m/z+1. Although we cannot rule out higher  
molecule fragmentation, interferences from other compounds are likely negligible for the masses presented in this study (Blake  
190 et al., 2009; Yuan et al., 2017). An exception could be isoprene, as it can contain fragments of 2-methyl-3-buten-2-ol (MBO)  
or cyclohexanes. However, during the period when the PTRMS measured in scan mode, MBO mass (m/z 87) was uncorrelated  
( $R^2= 0,02$ ) with m/z 69. In addition, the good correlation ( $R^2= 0.77$ ) between isoprene and Chl a across vertical profiles (Fig.  
S6) confirms that the measured m/z 69 can be mainly attributed to isoprene. For acetone, the signal corresponds to “acetone +  
propanal”, but propanal can be neglected and m/z 59 be considered as acetone (de Gouw and Warneke, 2007). The PTRMS  
195 used for this campaign was used the year before on a field campaign, and some of its characteristics are described in Zannoni

et al. (2016). The calibration procedures for gas and water phases are given in Supplement S4, Figures S4a and S4b. The measurement uncertainty is estimated at  $\pm 20\%$ , taking into account errors related to standard gas, calibrations, blanks, reproducibility and linearity (see S4). The overall uncertainty for dissolved VOC measurements was estimated at  $\pm 30\%$ , except for MeSH. Due to the missing direct calibration of MeSH, its concentration could be underestimated by up to 1.5 times  
200 (see S4). Therefore, reported concentrations presented here have to be considered as lower limit for MeSH.

### 2.3.2 CO measurements

CO was measured using a custom-made gas chromatograph directly coupled to the extraction cell, equipped with a hot mercuric-oxide detector operating at  $265^{\circ}\text{C}$  (RGA3, Trace Analytical, Menlo Park, CA, USA). The system comprised two 1-  
205 mL nominal volume stainless-steel injection loops for samples and calibration respectively, previously calibrated in the laboratory. The chromatographic procedure used a pre-column (0.77 m length, 0.32 cm outer diameter, containing Unibeads 1S 60/80 mesh) and an analytical column (0.77 m length, 0.32 cm outer diameter, containing molecular sieve 13X 60/80 mesh) both heated to  $95^{\circ}\text{C}$ . Air from the headspace of the extraction cell and standard gas were alternately injected into the chromatograph, each sample being directly calibrated with the previous injection of the standard gas. The standard gas  
210 consisted of CO diluted in synthetic air at a nominal concentration of 200 ppbv. The CO retention time was 1.5 min, and a complete chromatogram ran for 2.5 min. The overall accuracy of the measurement was about 5%. More details about CO measurements are described in Gros et al. (1999) and Tran et al. (2013).

## 3 Results

### 215 3.1 Latitudinal variability in surface waters from $57^{\circ}\text{N}$ to $80^{\circ}\text{N}$

Along the transect, the surface measurements of temperature, salinity and Chl a were performed across five different water masses: warm Atlantic Water with low salinity (AWs), 'regular' warm Atlantic Water (wAW), freshened and cooled Atlantic Water (fAW), cold Polar Water (cPW) and warm Polar Water (wPW) as defined in Table 1. The major part of the transect, from  $63$  to  $80^{\circ}\text{N}$ , occurred in wAW (Fig. 1). Atlantic Water with lower salinity (AWs and fAW) was encountered in the  
220 vicinity of the Norwegian Coastal Current (NCC) which carries water masses influenced by river run-off: AWs at  $60.6$ - $62.3^{\circ}\text{N}$  (with fAW in the mixing zones), and fAW around  $70$ - $72^{\circ}\text{N}$ . Fresher mixed products (fAW) were also intermittently encountered west of Svalbard (where AW meets fjord/coastal water masses), as well as in the marginal ice zone where AW mixes with and gradually subducts under fPW. Polar Water (PW) only occurred north of  $80^{\circ}\text{N}$  in the Nansen Basin. Surface temperature steadily decreased northwards, from  $8^{\circ}\text{C}$  to below  $0^{\circ}\text{C}$  in the ice-covered region  $>80^{\circ}\text{N}$  (Fig. 2). The slight  
225 deviation around  $70^{\circ}\text{N}$  corresponds to the shifting cruise track towards Tromsø due to a medical evacuation event (Fig. 1). Chl



a concentrations peaked at the beginning of the transect, with overall five areas where concentrations exceeded  $1 \mu\text{g L}^{-1}$  indicating increased phytoplankton abundances:  $\sim 60^\circ\text{N}$  to  $61^\circ\text{N}$  (up to  $2 \mu\text{g L}^{-1}$ ), several locations  $>66^\circ\text{N}$  ( $>6\text{-}8 \mu\text{g L}^{-1}$ ), and three peaks ( $>5 \mu\text{g L}^{-1}$ ) at  $76^\circ$ ,  $78^\circ$  and  $79.5^\circ\text{N}$ , respectively. Within the marginal ice zone ( $>80^\circ\text{N}$ ) Chl a concentrations reached up to  $3 \mu\text{g L}^{-1}$ .

### 230 3.1.1 Trace gas distribution

The oxygenated gases acetone and acetaldehyde strongly decreased with higher latitude and lower water temperature, being below or close to the detection limit north of  $70^\circ\text{N}$ . Nevertheless, we observed a 2- to 3-fold increase between  $61^\circ\text{N}$  and  $65^\circ\text{N}$ . Acetone varied from 20 to 25 nM between  $57$  to  $65^\circ\text{N}$ , decreasing to 0.1 nM near  $80^\circ\text{N}$ . A maximum of 40 nM between  $60^\circ\text{N}$  and  $65^\circ\text{N}$  covaried with higher Chl a concentrations, plus a second minor peak between  $77^\circ\text{N}$  and  $79^\circ\text{N}$ . Similar latitudinal trends occurred for acetaldehyde and acetonitrile. Acetaldehyde decreased from 15 nM in the temperate Atlantic to 0.5-3 nM in the Arctic Ocean, with a peak of approx. 40 nM between  $60^\circ\text{-}65^\circ\text{N}$ . Acetonitrile decreased from 1.5 nM to 0.1-0.5 nM, with a second maximum of approx. 2 nM between  $60^\circ$  and  $65^\circ\text{N}$ . Isoprene decreased from 4-5 pM at  $57^\circ\text{N}$  to 0.3-1.5 pM at  $80^\circ\text{N}$ , with three additional maxima along the transect. Opposed to the other trace gases, isoprene slightly increased again north of  $80^\circ\text{N}$ , albeit at a much lower concentration compared to lower latitudes.

240

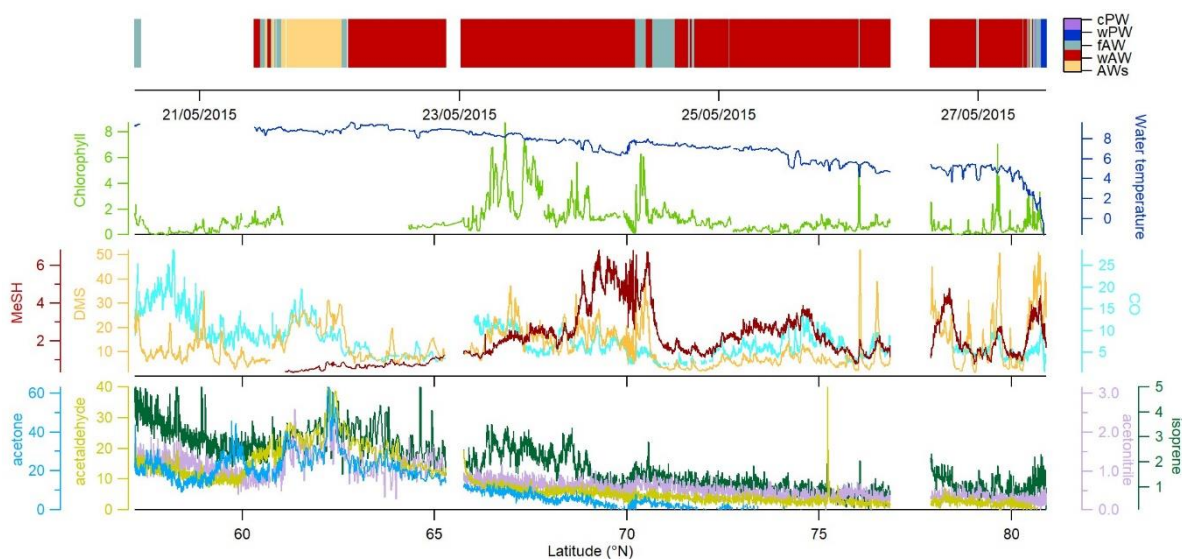


**Fig. 2:** Latitudinal variability of acetone (nM), acetaldehyde (nM), acetonitrile (nM), isoprene (pM), DMS (nM), MeSH (nM), and CO (nM) between  $57.2^\circ\text{N}$  to  $80.9^\circ\text{N}$  in relation to Chl a ( $\mu\text{g L}^{-1}$ ) and water temperature ( $^\circ\text{C}$ ). Due to sensor failure temperature records are missing until  $\sim 61^\circ\text{N}$ . The colored horizontal bar on top illustrates the encountered water masses (Fig. 1). Values below 3 nM are below the detection

245 limit for acetone and acetaldehyde (see S4).

CO, DMS and MeSH displayed different patterns, retaining high but variable concentrations at high latitudes. CO concentrations varied between 2 and 30 nM, with several peaks covarying with Chl a at 62.5, 67 and 77.6°N. DMS ranged from ~2 nM to 50 nM, with peaks at 61-63°N, 66-70.5°N and a maximum of 60 nM at 80°N. MeSH varied from 0.1 to 7 nM, with peaks near 70°N and between 73-75°N.

### 3.1.2 Bacterial communities in the environmental context

We performed 16S rRNA amplicon sequencing to characterize bacterial community structure in context of latitude, water temperature and trace gas concentrations. Correspondent to the known microbial differences between temperate and polar oceans (Sunagawa et al., 2015), communities substantially varied by latitude and temperature. These factors explained 43% of bacterial variability (PERMANOVA;  $p < 0.001$ ). Accordingly, communities markedly varied between Atlantic and polar waters >80°N (Fig. 3a). Several correlations between trace gases, Chl a and the abundance of specific ASVs (Fig. 3b) suggests bacterial linkages with phytoplankton and VOC dynamics. Correlations were both positive and negative, sometimes differing within single genera. For instance, one SAR92-ASV positively correlated with MeSH, whereas another SAR92-ASV negatively correlated with DMS. For MeSH and its ratio to DMS, correlations differed between *Pseudofulvibacter*, NS10, OM75, *Yoonia-Loktanella* and *Asciadiaceihabitans* ASVs (negative) versus SUP05 (positive). *Synechococcus* and an unclassified cyanobacterial ASV were negatively correlated with MeSH. DMS positively correlated with ASVs from *Aurantivirga* and SAR11 clade Ia. Two ASVs from the NS9 clade were unique in their correlations with acetone and acetonitrile. Furthermore, several ASVs from *Thalassolituus* and *Alcanivorax* (negative), NS5 and *Polaribacter* (positive) correlated with Chl a and isoprene.

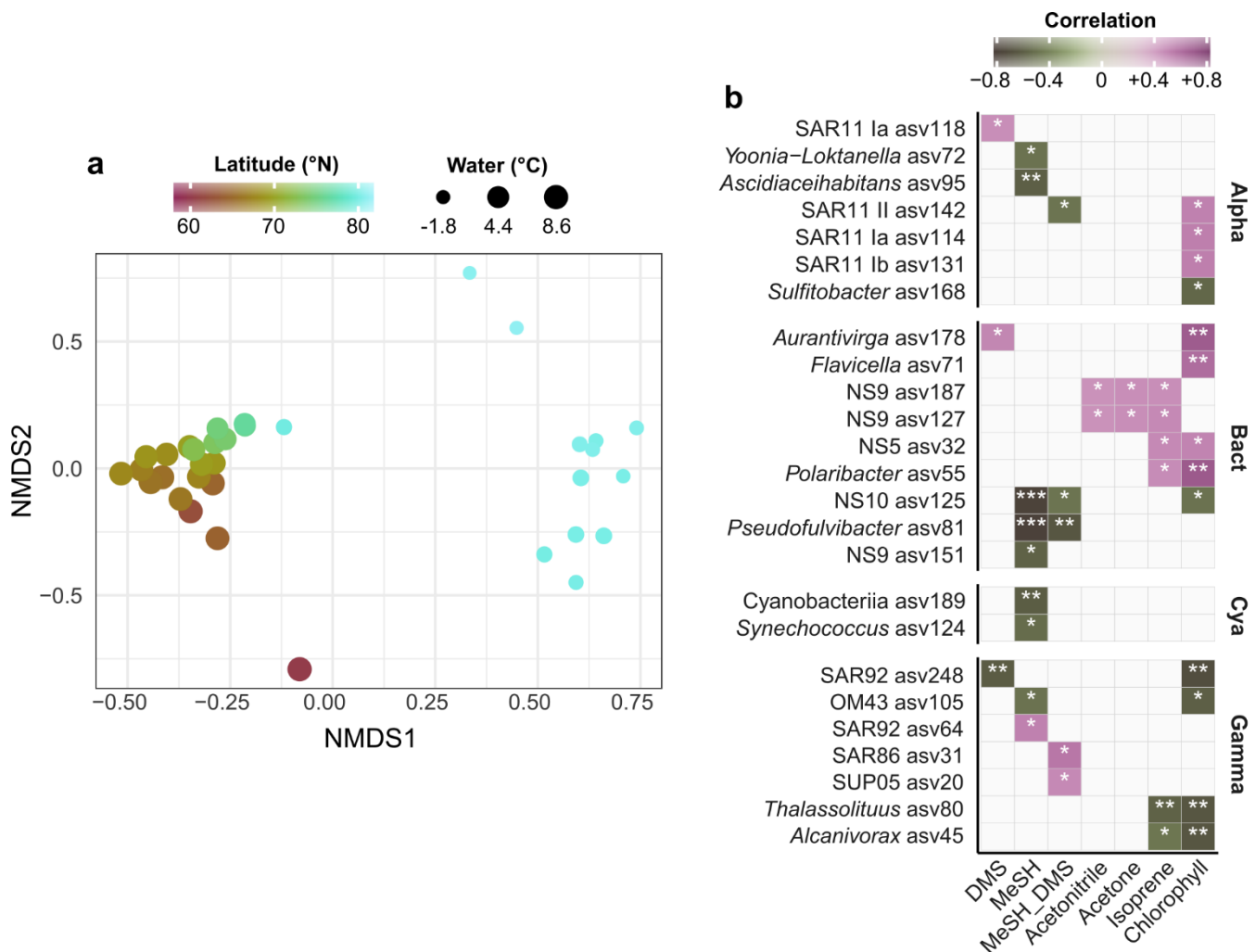


**Fig. 3.** a) Nonmetric multidimensional scaling of bacterial community composition (Bray-Curtis dissimilarities of Hellinger-transformed relative abundances). The colour gradient and dot size illustrate latitude and water temperature respectively. b) Spearman correlations between environmental parameters and the abundance of bacterial ASVs. MeSH\_DMS: ratio between MeSH and DMS, expressed as MeSH/(MeSH+DMS). Only correlations  $>|0.4|$  are shown, and only if stronger than with latitude. No correlations occurred with acetaldehyde and CO. Alpha: Alphaproteobacteria; Gamma: Gammaproteobacteria; Bact: Bacteroidetes; Cya: Cyanobacteria. Asterisks indicate Holm-corrected  $p$  values (\*  $< 0.05$ ; \*\*  $< 0.01$ ; \*\*\*  $< 0.001$ ).

### 3.2 Vertical under-ice profiles north of 80°N

In the ice-covered region north of Svalbard, we performed vertical under ice profiles at eight stations instead of the continuous surface seawater measurements (Fig. 1, Fig. 4, Fig. S5, section 2.1). To connect latitudinal and vertical records, we compared the cPW values measured along the transect with the surface values (0.5 m depth) from the vertical profiles (Tab. 1, Fig. 4).

This revealed marked differences in trace gas concentrations compared to polar water masses along the transect, except for acetonitrile. Acetaldehyde concentrations (0.3 to 14.2 nM with an average of  $7.2 \pm 4.4$  nM) were much higher than in polar waters along the transect ( $0.8 \pm 2.0$  nM), and more in the range of the previously described wAW ( $4.8 \pm 4.0$  nM) and fAW ( $9.8 \pm 5.6$  nM). A similar increase was apparent for acetone, with values closer to wAW than to polar waters. DMS varied substantially (1.6 to 31.9 nM) at the sea-ice stations. DMS concentrations at the bloom stations 19 and 32 (see section 2.1 and Fig. 4) were similar as in polar waters along the transect, whereas the pre-bloom stations (39, 43, 46) only showed  $>2$  nM DMS at 0.5 m depth. MeSH and CO both exhibited lower concentrations ( $0.13 \pm 0.17$  nM and  $1.45 \pm 1.67$  nM respectively) at the sea-ice stations. In contrast, isoprene concentrations were higher ( $3.2 \pm 2.1$  pM) at the sea-ice stations compared to all other water masses along the transect. The substantial difference between polar waters observed in the northern part of the transect and surface values waters from sea-ice stations was also evident in Chl a, marker pigments of relevant phytoplankton groups (diatoms and *Phaeocystis*), and some trace gases (DMS, MeSH, CO, isoprene).

The shallow shelf stations 19 and 32 featured a marked phytoplankton bloom, with up to  $10 \mu\text{g L}^{-1}$  of Chl a. The predominance of diatoms, constituting 90% of phytoplankton illustrates a typical spring bloom scenario (Degerlund and Eilertsen, 2010). Station 27, 31 and 47 had roughly 50% diatom contribution while the pre-bloom stations 39, 43 and 46 were characterized by a mixed pico- and nanophytoplankton community of prasinophytes, chlorophytes, dinoflagellates, cryptophytes, chrysophytes and coccolithophorid-type haptophytes (Fig. S5) and Chl a  $< 0.5 \mu\text{g L}^{-1}$ . *Phaeocystis*, a typical bloom-forming organism in the High Arctic (Degerlund and Eilertsen, 2010), constituted up to 80% of the phytoplankton biomass at station 47, but their biomass concentration was much lower compared to the *Phaeocystis* under-ice bloom found in the same region and year (Assmy et al., 2017). This indicates a declining bloom during our sampling period. Except for the Yermak plateau stations (39, 43, 46), *Phaeocystis* contributed between 10-40% of the phytoplankton biomass.

DMS and Chl a were strongly correlated ( $R^2$  Pearson's correlation coefficient = 0.93; Fig. S6). Isoprene also correlated with Chl a ( $R^2 = 0.6$ , Fig. S6) but only when excluding station 19. This correlation supports a biological source of isoprene, in agreement with previous demonstrated links between isoprene and Chl a maxima (Tran et al., 2013). Station 19 was the only station where diatoms almost exclusively dominated the phytoplankton biomass. The little emission of isoprene by cold-water diatoms (Bonsang et al., 2010) could explain this pattern.

In contrast to the latitudinal transect, MeSH showed low concentrations at most ice stations, with the exception of station 19. Station 19 was special due to its location above the shelf, and the phytoplankton community dominated by diatoms.

CO concentrations overall decreased with depth (Tran et al., 2013), except for station 31 with a CO peak at 30 m depth.

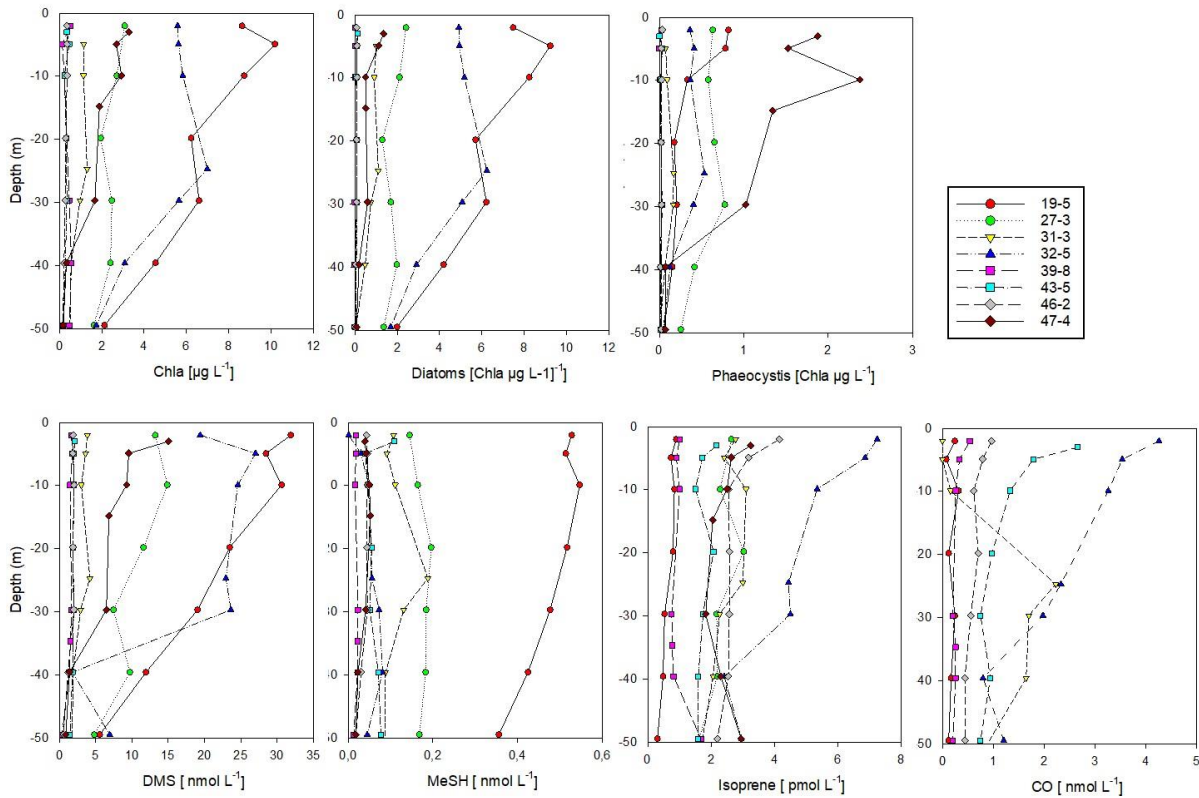


**Fig. 4.** Vertical profiles of biological parameters and trace gas concentrations (0-50 m depth) at sea-ice covered stations north of 80°. According to Dybwad et al., (2021) stations 39, 43 and 46 (Yermak Plateau) were in a pre-bloom phase, while all other stations were in a bloom phase. Stations 19 and 32 were shelf stations. The contribution of each phytoplankton group is expressed as Chl a concentration.

## 4 Discussion

### 4.1 Isoprene, CO, acetone, acetaldehyde and acetonitrile

Our study provides a comprehensive overview of biologically and climatically relevant trace gases in the microbiological context; covering ~1400 nautical miles from 57°N to 81°N, as well as under-ice vertical profiles north of Svalbard, in May-June 2015. Isoprene and CO concentrations can be compared with a previous study carried out in June-July 2010 (Tran et al., 2013), i.e. one month later in summer and in different water masses (Table 1) but where only few phytoplankton blooms were encountered.

320

**Table 1:** Mean values and standard deviation for concentration of trace gases in five different water masses along the transect (see Fig. 1 for exact areas), and from surface samples at eight sea-ice stations north of 80°N. S: salinity; BDL: below detection limit. \*In italics: data from (Tran et al., 2013) in the same area but in June-July 2010, i.e. one month later in summer. Due to sensor failure of temperature and salinity, the records start at 60°N.

	Acetonitrile (nM)	Acetaldehyde (nM)	Acetone (nM)	DMS (nM)	Methanethiol (nM)	MeSH/(Me SH+DMS) %	Isoprene (pM)	CO (nM)
Coastal- influenced/low- salinity Atlantic Water (AWs; $\theta > 5^\circ\text{C}$ , $S < 34.4$ )	$1.11 \pm 0.55$	$19.67 \pm 7.96$	$23.34 \pm 12.77$	$15,65 \pm 6.96$	$0.84 \pm 0.65$	$5.6 \pm 7.1$	$2,55 \pm 0.84$ <i>23.4 ± 3.10*</i>	$10.70 \pm 3.07$ <i>2.50 ± 1.70*</i>
warm Atlantic Water (wAW; $\theta > 2^\circ\text{C}$ , $S > 34.9$ )	$0.53 \pm 0.23$	$4.84 \pm 4.03$	$2.36 \pm 5.88$	$11,75 \pm 6.97$	$2.89 \pm 1.52$	$21.9 \pm 8.7$	$1,38 \pm 0.70$ <i>42.5 ± 49.6*</i>	$5.86 \pm 2.77$ <i>3.3 ± 2.2*</i>
freshened Atlantic Water (fAW; $\theta > 1^\circ\text{C}$ , $34.4 < S < 34.9$ )	$0.94 \pm 0.40$	$9.84 \pm 5.60$	$14.56 \pm 10.80$	$13.05 \pm 8.83$	$3.26 \pm 1.49$	$20.7 \pm 10.6$	$2,66 \pm 1.51$ <i>24.8. ± 19.1*</i>	$10.17 \pm 5.89$ <i>3.4 ± 2.4*</i>
cold Polar Water (cPW; $\theta < 0^\circ\text{C}$ , $S < 34.7$ )	$0.32 \pm 0.13$	$0.98 \pm 2.27$	BDL	$30.03 \pm 9.26$	$2.80 \pm 0.76$	$9.1 \pm 2.3$	$1,22 \pm 0.47$	$5.00 \pm 2.82$
warm Polar Water (wPW; $\theta > 0^\circ\text{C}$ , $S < 34.4$ )	$0.21 \pm 0.09$	$0.30 \pm 0.86$	BDL	$34.65 \pm 8.46$	$3.49 \pm 0.29$	$9.6 \pm 2.0$	$1,06 \pm 0.28$	$7.81 \pm 2.08$
Polar waters (PW) (cold+warm)	$0.30 \pm 0.13$	$0.84 \pm 2.05$	BDL	$31.19 \pm 9.29$	$2.96 \pm 0.74$	$9.2 \pm 2.2$	$1,19 \pm 0.44$ <i>14.5 ± 11.5*</i>	$5.88 \pm 2.91$ <i>6.5 ± 3.2*</i>
Surface water at sea-ice stations > 80°N (range)	$0.28 \pm 0.12$ (0.15-0.47)	$7.24 \pm 4.43$ (0.27-14.23)	$2.29 \pm 2.79$ (0-6.93)	$11.22 \pm 10.91$ (1.64-31.90)	$0.13 \pm 0.17$ (0.02-0.53)		$3.23 \pm 2.07$ (0.90-7.25)	$1.45 \pm 1.67$ (0.24-4.26)

The concentrations of isoprene reported here, usually associated with phytoplankton (Bonsang et al., 1992; Shaw et al., 2010), were about one order of magnitude lower than described by Tran et al. (2013), even though the biomass indicator Chl a was overall lower ( $2 \mu\text{g L}^{-1}$  compared to up to  $8 \mu\text{g L}^{-1}$  reported here). This may relate to seasonal differences in phytoplankton composition, as phytoplankton taxa are known to vary their isoprene emissions (Bonsang et al., 2010; Shaw et al., 2010). Similar seasonal differences in isoprene concentrations were observed by Hackenberg et al., (2017), reporting on average 4.3 pM for March compared to 19.9 pM in July/August in the Arctic sector of the Pacific Ocean. Lower isoprene concentrations in polar waters correspond to Ooki et al. (2015), who found 27 – 33 pM in subpolar and transition waters and 4 pM in polar waters, respectively. With regard to vertical profiles, the slight secondary maximum at 20-40 m depth may correspond to the Chl a maximum, as reported by Tran et al. (2013). Nevertheless, the concentrations in our study are overall much lower (about one order of magnitude) than reported by Tran et al., (2013), indicating a high spatial variability of isoprene potentially related to seasonally varying phytoplankton abundances. Simó et al., (2022) recently highlighted the importance of biological consumption of isoprene in water, possibly matching the magnitude of isoprene ventilated to the atmosphere, advising to consider both the sources and sinks when discussing isoprene concentrations and variability. The correlations of *Alcanivorax* and *Thalassolituus* ASVs with both isoprene and Chl a support phytoplankton as source of this trace gas. *Alcanivorax* has been reported during phytoplankton blooms in the subarctic Atlantic (Thompson et al., 2020) and can degrade isoprene (Alvarez et al., 2009). *Alcanivorax* and *Thalassolituus* can be associated with microalgal surfaces and also perform hydrocarbon degradation (Love et al., 2021), indicating additional phytoplankton-linked factors that influence their distribution.

To date, CO in Arctic seawater has only been measured by Tran et al. (2013) in the same Arctic region, as well as by Xie and Zafiriou (2009) in the Beaufort Sea. The mean concentration of  $5.9 \pm 2.9$  nM in polar waters along the transect matches previously reported averages ( $6.5 \pm 3.2$  nM for Tran et al. (2013) and  $4.7 \pm 2.4$  nM for Xie and Zafiriou (2009), respectively). These concentrations are relatively high compared to the global oceanic mean of 2 nM CO (Conte et al., 2019). Elevated values in the Arctic are not reproduced by the NEMO-PISCES model (Conte et al., 2019), which might be caused by the bio-optical relationship between coloured dissolved organic matter (CDOM) and Chl a. NEMO-PISCES was originally developed for typical oceanic waters (Morel and Gentili, 2009). However, Arctic waters do not conform to this bio-optical type and are considered optically complex waters, with distinct signatures of CDOM and particle loads through the interplay of oceanic, riverine and ice-melt waters (Gonçalves-Araujo et al., 2018). Conte et al. (2019) attribute the release of CO and/or CDOM to sea-ice melt or to a lower bacterial consumption in cold waters. The first hypothesis is supported by up to 100 nM CO measured in sea ice (Xie and Gosselin, 2005; Song et al., 2011). Concerning CO in Atlantic waters, concentrations of up to  $10.7 \pm 3.1$  nM are higher than in polar waters, and exceed data from the same region measured 5 years earlier (Tran et al., 2013) by up to four times. Highest CO values in temperate waters with low Chl a suggest that CO originated from an abiotic source, e.g. the photodegradation of CDOM. Even in the ice covered waters the strong reduction with depth supports the notion that CO photoproduction decreases up to three times from the surface to 20 m depth (Fichot and Miller, 2010). But in some vertical under-ice profiles, similar trajectories of Chl a and CO suggest an additional biological source, as shown by Tran et al. (2013).

Biological sources of CO have been extensively studied by Gros et al., (2009), and the missing congruency at station 19 could be explained by the relatively low CO emission of cold-water diatoms (Gros et al. 2009), since diatoms accounted for the large bloom at the shelf station 19 (Fig. 3).

365 Considerable differences between Atlantic and polar waters occurred for acetone, acetonitrile and acetaldehyde. Reference data on acetone concentrations are scarce (Beale et al., 2013; Tanimoto et al., 2014; Wohl et al., 2020 and references therein), and report 2 to 40 nM in the temperate and tropical Atlantic (Williams et al., 2004) as well as west Pacific Oceans (Marandino, 2005). In the Atlantic Ocean, Yang et al., (2014) observed a mean value of 13.7 nM, without an obvious correlation to biological activity. For the Arctic Ocean, Yang et al. (2014) reported 6.8 nM in the Labrador Sea and Wohl et al. (2019)  $8 \pm 2$  nM in the Canadian Arctic, matching our data between 65-70°N. Notably, these patterns match the southern Atlantic at 60°S (Wohl et al., 2020), suggesting similar dynamics in both subpolar regions. For acetone, the ocean is considered to be both a photochemical source and a microbial sink depending on the region (Jacob et al., 2002; Fischer et al., 2012). This dual role matches there herein observed relatively high values >60°N, and values down to the detection limit in polar zones. For acetonitrile, the oceans are a comparatively small source (originating from phytoplankton) or sink (through bacterial consumption) depending on location and season (see Singh (2003); Williams et al., (2004) and references therein). The concentrations measured in the present study were mostly >1 nM, and to our knowledge, the first reported in the Arctic Ocean. 370 Overall, little is known about microbial utilization of acetone and acetonitrile, but biogenic effects have been suggested (Davie-Martin et al. (2020). Correlations of the NS9 clade (Flaobacteriales) with acetone and acetonitrile indicate an involvement in acetone and acetonitrile cycling among this diverse uncultured taxon.

Prior acetaldehyde measurements (Zhou and Mopper, 1997; Kameyama et al., 2010; Yang et al., 2014) reported 1.5 to 5 380 nM in the North Atlantic Ocean. In the present study, concentrations in AWs ( $19.7 \pm 8.0$  nM) were on average two times higher than those found in the North Atlantic by Yang et al. (2014) and Zhu and Kieber (2019). However, these related studies measured acetaldehyde in autumn, which could explain the difference as the main source of acetaldehyde is attributed to photochemical degradation of CDOM.

## 385 4.2 DMS and MeSH

Previously reported DMS concentrations in polar oceans varied between 3 to 18 nM (Mungall et al., 2016; Jarníková et al., 2018; Uhlig et al., 2019), with up to 74 nM in the sub-surface Chl a maximum of Baffin Bay (Galí et al., 2021). Hence, these are overall in the same range as our values. The average around 30 nM observed north of 80°N might be partly explained by the high DMS concentrations (up to 2000 nM) in sea ice (Levasseur, 2013; see also Hayashida et al., 2020). Indeed, ice-melt derived DMS can contribute up to 50% to the water column inventory (Tison et al., 2010). 390

Stefels et al. (2007) have suggested no direct relationship between DMS and Chl a on a global scale, since the precursor of DMS (DMSP) is produced by diverse phytoplankton at different rates, connected to their physiological state. However, different approaches employed by Gali et al. (2018) and Wang et al. (2020) have shown that Chl a can be a strong predictor of



DMS concentrations. In addition, reported that the DMS-Chl a correlation strongly varies with latitude, with a positive  
395 correlation at high latitudes (north of 40°N and south of 40°S). Nevertheless, we note that the figure presented by Lana et al.  
(2012) shows a lower correlation on the region covered by our transect. The missing correlation found along our transect ( $R^2$   
=0.1) likely reflects different phytoplankton types and bloom stages (Dybwad et al., 2021), whereas the strong correlation  
between Chl a and DMS in the Atlantic-influenced polar water masses at vertical under-ice profiles mirrored observations by  
Uhlig et al. (2019). Presumably, this is a typical marginal sea ice zone effect, as found in other sectors of the Arctic (Galí and  
400 Simó, 2010; Levasseur, 2013; Park et al., 2013).

Compared to DMS, MeSH has seldom been quantified in marine waters to date, especially at polar latitudes. Leck  
and Rodhe (1991) reported on average 0.16 nM MeSH in the Baltic Sea, and 0.28 nM and 0.34 nM in the North Sea  
respectively. Our data are one order of magnitude higher, ranging from  $0.84 \pm 0.65$  nM in AWs to 3.49 nM in wPW, i.e. in the  
same range observed by Kiene et al. (2017) in the northeast subarctic Pacific Ocean. These authors showed that MeSH  
405 concentrations in surface waters generally decrease with depth, a feature which generally matches our under-ice vertical  
profiles although concentrations were low.

MeSH and DMS originate from the degradation of DMSP, mostly via bacterial demethylation (yielding MeSH) or  
cleavage (yielding DMS) (Moran and Durham, 2019; Lawson et al., 2020 and references therein). Laboratory experiments  
have indicated that the net yields of DMS and MeSH from DMSP were on average 32% and 22% respectively (Kiene, 1996).  
410 MeSH production might be promoted by low DMSP concentrations and high bacterial sulphur demand (Kilgour et al., 2022).  
Mesocosm experiments showed that the proportion of DMS versus MeSH increased from the pre-bloom phase to (induced)  
bloom conditions (Kilgour et al., 2022). In pelagic waters, DMS generally dominates gaseous sulphur, with MeSH being the  
second most abundant compound contributing on average  $\leq 15\%$  to the total sulphur species in the North and Baltic seas (Leck  
and Rodhe, 1991), in the Atlantic Ocean (Kettle et al., 2001), and in the Southwest Pacific Ocean (Lawson et al., 2020).

415 Comparable to some North Sea locations (Leck and Rodhe, 1991), MeSH contributed up to 40% between 70°N-75°N  
in our study, with a maximum of 50% at 78.6°N (Fig. 5a). This latitudinal variability was underlined by shifts in major bacterial  
genera. For instance, *Paraglaucicola* (Gammaproteobacteria) and NS4 (Bacteroidetes) peaked together with the highest MeSH  
fraction between 70-80°N. *Amylibacter* decreased towards the north, whereas unclassified *Nitrincolaceae* prevailed north of  
80°N together with an again smaller MeSH/DMS ratio (Fig. 5b). The overall MeSH contribution of 20% suggests that MeSH  
420 represents a considerable fraction of sulphur, with linkages to microbial dynamics. Accordingly, we found several correlations  
with the abundance of specific ASVs. Correlations between *Yoonia-Loktanella* and *Ascidiahabitans* ASVs with MeSH  
reflect the prominent role of *Rhodobacteraceae* in DMSP demethylation (Curson et al., 2011; Moran et al., 2012). The positive  
relation of SAR11 and SUP05 ASVs corresponds to the prevalence of DMSP-metabolizing genes in these taxa (Nowinski et  
al., 2019; Landa et al., 2019; Sun et al., 2016). The link between cyanobacteria and MeSH potentially relates to the known

425 uptake of DMSP by *Synechococcus* and *Prochlorococcus* (Vila-Costa et al., 2006), although DMSP-utilizing genes are overall rare in cyanobacteria (Liu et al., 2018). Overall, there could be yet undescribed chemical linkages among primary producers.

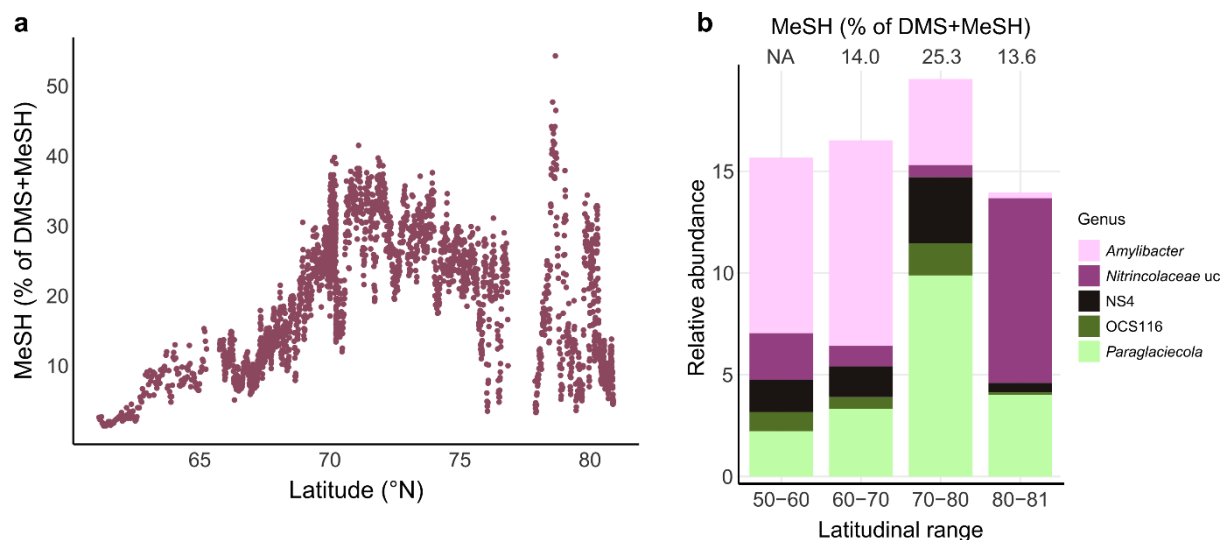


Fig. 5: MeSH contribution to the sulphur budget and associated bacterial patterns.: Latitudinal variation of the MeSH fraction  
430 to the total sulphur compounds measured (DMS+MeSH). b: Relative abundance of selected bacterial genera by latitudinal  
range and the corresponding MeSH/DMS ratio. NA: not available; uc: unclassified.

## 5 Conclusion

We present the first measurements of DMS, MeSH and other trace gases along a transect from the North Atlantic to  
435 the ice-covered Arctic Ocean. High-resolution latitudinal data between 57°N and 80°N were complemented with vertical  
profiles at sea-ice stations north of 80°N. Whereas isoprene, acetone, acetaldehyde and acetonitrile concentrations decreased  
northwards, CO, DMS and MeSH were uncorrelated with latitude and retained considerable concentrations in polar waters.  
Hence, these likely have phytoplankton-driven origins with regional variability, e.g. through localized blooms and/or the  
presence of sea-ice. The DMS peak in polar waters pointed to sea ice as reservoir of DMS (Levasseur, 2013) and the prevalence  
440 of DMS-emitting phytoplankton. The marked correlation between DMS and Chl a in the diatom-dominated region north of  
80°N represented a typical marginal sea ice zone effect. The missing correlation between DMS and MeSH suggested different  
processes of production and degradation, although both compounds originate from DMSP. Although DMS was overall more  
abundant, MeSH contributed on average 20% (and up to 50%) to the total DMS+MeSH budget, suggesting consideration of

MeSH as secondary aerosol producer in some regions. The potential importance of MeSH was underlined by more and stronger  
445 bacterial correlations than with DMS, indicating that bacterial DMSP demethylation is important across extensive latitudinal  
gradients. Notably, higher acetaldehyde concentrations north of 80°N suggests that ice-covered regions could be a reservoir of  
acetaldehyde. While artefacts from off-line measurements (sampling through Niskin bottles) cannot be completely excluded,  
this result indicates a potential role of this reactive compound in regional atmospheric chemistry. However, a comprehensive  
understanding of marine trace gas dynamics, including the rapidly changing Arctic, requires further measurements in seawater,  
450 sea-ice and atmosphere. In conclusion, the reported trace gas concentrations in high spatial resolution provide important  
insights into climatically and biologically relevant compounds and their connection to microbiology.

## References

- Alvarez, L. A., Exton, D. A., Timmis, K. N., Suggett, D. J., and McGenity, T. J.: Characterization of marine isoprene-degrading  
communities, *Environmental Microbiology*, 11, 3280–3291, <https://doi.org/10.1111/j.1462-2920.2009.02069.x>, 2009.
- 455 von Appen, W.-J., Waite, A. M., Bergmann, M., Bienhold, C., Boebel, O., Bracher, A., Cisewski, B., Hagemann, J., Hoppema,  
M., Iversen, M. H., Konrad, C., Krumpfen, T., Lochthofen, N., Metfies, K., Niehoff, B., Nöthig, E.-M., Purser, A., Salter, I.,  
Schaber, M., Scholz, D., Soltwedel, T., Torres-Valdes, S., Wekerle, C., Wenzhöfer, F., Wietz, M., and Boetius, A.: Sea-ice  
derived meltwater stratification slows the biological carbon pump: results from continuous observations, *Nat Commun*, 12,  
7309, <https://doi.org/10.1038/s41467-021-26943-z>, 2021.
- 460 Arrigo, K. R. and van Dijken, G. L.: Continued increases in Arctic Ocean primary production, *Progress in Oceanography*, 136,  
60–70, <https://doi.org/10.1016/j.pocean.2015.05.002>, 2015.
- Assmy, P., Fernández-Méndez, M., Duarte, P., Meyer, A., Randelhoff, A., Mundy, C. J., Olsen, L. M., Kauko, H. M., Bailey,  
A., Chierici, M., Cohen, L., Doulgeris, A. P., Ehn, J. K., Fransson, A., Gerland, S., Hop, H., Hudson, S. R., Hughes, N., Itkin,  
P., Johnsen, G., King, J. A., Koch, B. P., Koenig, Z., Kwasniewski, S., Laney, S. R., Nicolaus, M., Pavlov, A. K., Polashenski,  
465 C. M., Provost, C., Rösel, A., Sandbu, M., Spreen, G., Smedsrud, L. H., Sundfjord, A., Taskjelle, T., Tatarek, A., Wiktor, J.,  
Wagner, P. M., Wold, A., Steen, H., and Granskog, M. A.: Leads in Arctic pack ice enable early phytoplankton blooms below  
snow-covered sea ice, *Sci Rep*, 7, 40850, <https://doi.org/10.1038/srep40850>, 2017.
- Beale, R., Dixon, J. L., Arnold, S. R., Liss, P. S., and Nightingale, P. D.: Methanol, acetaldehyde, and acetone in the surface  
waters of the Atlantic Ocean: OVOCs in The Atlantic Ocean, *J. Geophys. Res. Oceans*, 118, 5412–5425,  
470 <https://doi.org/10.1002/jgrc.20322>, 2013.
- Bikkina, S., Kawamura, K., Miyazaki, Y., and Fu, P.: High abundances of oxalic, azelaic, and glyoxylic acids and  
methylglyoxal in the open ocean with high biological activity: Implication for secondary OA formation from isoprene: Oceanic  
control on atmospheric SOA, *Geophys. Res. Lett.*, 41, 3649–3657, <https://doi.org/10.1002/2014GL059913>, 2014.
- Blake, R. S., Monks, P. S., and Ellis, A. M.: Proton-Transfer Reaction Mass Spectrometry, *Chem. Rev.*, 109, 861–896,  
475 <https://doi.org/10.1021/cr800364q>, 2009.
- Bonsang, B., Polle, C., and Lambert, G.: Evidence for marine production of isoprene, *Geophys. Res. Lett.*, 19, 1129–1132,  
<https://doi.org/10.1029/92GL00083>, 1992.

- 480 Bonsang, B., Gros, V., Peeken, I., Yassaa, N., Bluhm, K., Zoellner, E., Sarda-Esteve, R., and Williams, J.: Isoprene emission from phytoplankton monocultures: the relationship with chlorophyll-a, cell volume and carbon content, *Environ. Chem.*, 7, 554, <https://doi.org/10.1071/EN09156>, 2010.
- Butkovskaya, N. I. and Setser, D. W.: Product Branching Fractions and Kinetic Isotope Effects for the Reactions of OH and OD Radicals with CH<sub>3</sub>SH and CH<sub>3</sub>SD, *J. Phys. Chem. A*, 103, 6921–6929, <https://doi.org/10.1021/jp9914828>, 1999.
- Callahan, B. J., McMurdie, P. J., Rosen, M. J., Han, A. W., Johnson, A. J. A., and Holmes, S. P.: DADA2: High-resolution sample inference from Illumina amplicon data, *Nat Methods*, 13, 581–583, <https://doi.org/10.1038/nmeth.3869>, 2016.
- 485 Campen, H. I., Arévalo-Martínez, D. L., Artioli, Y., Brown, I. J., Kitidis, V., Lessin, G., Rees, A. P., and Bange, H. W.: The role of a changing Arctic Ocean and climate for the biogeochemical cycling of dimethyl sulphide and carbon monoxide, *Ambio*, 51, 411–422, <https://doi.org/10.1007/s13280-021-01612-z>, 2022.
- Carrión, O., McGenity, T. J., and Murrell, J. C.: Molecular Ecology of Isoprene-Degrading Bacteria, *Microorganisms*, 8, 967, <https://doi.org/10.3390/microorganisms8070967>, 2020.
- 490 Charlson, R. J., Lovelock, J. E., Andreae, M. O., and Warren, S. G.: Oceanic phytoplankton, atmospheric sulphur, cloud albedo and climate, *Nature*, 326, 655–661, <https://doi.org/10.1038/326655a0>, 1987.
- Ciuraru, R., Fine, L., Pinxteren, M. van, D’Anna, B., Herrmann, H., and George, C.: Unravelling New Processes at Interfaces: Photochemical Isoprene Production at the Sea Surface, *Environ. Sci. Technol.*, 49, 13199–13205, <https://doi.org/10.1021/acs.est.5b02388>, 2015.
- 495 Conte, L., Szopa, S., Séférian, R., and Bopp, L.: The oceanic cycle of carbon monoxide and its emissions to the atmosphere, *Biogeosciences*, 16, 881–902, <https://doi.org/10.5194/bg-16-881-2019>, 2019.
- Curson, A. R. J., Todd, J. D., Sullivan, M. J., and Johnston, A. W. B.: Catabolism of dimethylsulphoniopropionate: microorganisms, enzymes and genes, *Nat Rev Microbiol*, 9, 849–859, <https://doi.org/10.1038/nrmicro2653>, 2011.
- 500 Davie-Martin, C. L., Giovannoni, S. J., Behrenfeld, M. J., Penta, W. B., and Halsey, K. H.: Seasonal and Spatial Variability in the Biogenic Production and Consumption of Volatile Organic Compounds (VOCs) by Marine Plankton in the North Atlantic Ocean, *Front. Mar. Sci.*, 7, 611870, <https://doi.org/10.3389/fmars.2020.611870>, 2020.
- Degerlund, M. and Eilertsen, H. C.: Main Species Characteristics of Phytoplankton Spring Blooms in NE Atlantic and Arctic Waters (68–80° N), *Estuaries and Coasts*, 33, 242–269, <https://doi.org/10.1007/s12237-009-9167-7>, 2010.
- 505 Duncan, B. N., Logan, J. A., Bey, I., Megretskaia, I. A., Yantosca, R. M., Novelli, P. C., Jones, N. B., and Rinsland, C. P.: Global budget of CO, 1988–1997: Source estimates and validation with a global model, *J. Geophys. Res.*, 112, D22301, <https://doi.org/10.1029/2007JD008459>, 2007.
- Dybwad, C., Assmy, P., Olsen, L. M., Peeken, I., Nikolopoulos, A., Krumpfen, T., Randelhoff, A., Tatarek, A., Wiktor, J. M., and Reigstad, M.: Carbon Export in the Seasonal Sea Ice Zone North of Svalbard From Winter to Late Summer, *Front. Mar. Sci.*, 7, 525800, <https://doi.org/10.3389/fmars.2020.525800>, 2021.
- 510 Fernández-Méndez, M., Wenzhöfer, F., Peeken, I., Sørensen, H. L., Glud, R. N., and Boetius, A.: Composition, Buoyancy Regulation and Fate of Ice Algal Aggregates in the Central Arctic Ocean, *PLoS ONE*, 9, e107452, <https://doi.org/10.1371/journal.pone.0107452>, 2014.

- 515 Fichot, C. G. and Miller, W. L.: An approach to quantify depth-resolved marine photochemical fluxes using remote sensing: Application to carbon monoxide (CO) photoproduction, *Remote Sensing of Environment*, 114, 1363–1377, <https://doi.org/10.1016/j.rse.2010.01.019>, 2010.
- Fischer, E. V., Jacob, D. J., Millet, D. B., Yantosca, R. M., and Mao, J.: The role of the ocean in the global atmospheric budget of acetone: ATMOSPHERIC BUDGET OF ACETONE, *Geophys. Res. Lett.*, 39, n/a-n/a, <https://doi.org/10.1029/2011GL050086>, 2012.
- 520 Galí, M. and Simó, R.: Occurrence and cycling of dimethylated sulfur compounds in the Arctic during summer receding of the ice edge, *Marine Chemistry*, 122, 105–117, <https://doi.org/10.1016/j.marchem.2010.07.003>, 2010.
- Galí, M., Lizotte, M., Kieber, D. J., Randelhoff, A., Hussherr, R., Xue, L., Dinasquet, J., Babin, M., Rehm, E., and Levasseur, M.: DMS emissions from the Arctic marginal ice zone, *Elementa: Science of the Anthropocene*, 9, 00113, <https://doi.org/10.1525/elementa.2020.00113>, 2021.
- 525 Galindo, V., Levasseur, M., Mundy, C. J., Gosselin, M., Tremblay, J.-É., Scarratt, M., Gratton, Y., Papakiriakou, T., Poulin, M., and Lizotte, M.: Biological and physical processes influencing sea ice, under-ice algae, and dimethylsulfoniopropionate during spring in the Canadian Arctic Archipelago, *J. Geophys. Res. Oceans*, 119, 3746–3766, <https://doi.org/10.1002/2013JC009497>, 2014.
- GEBCO Bathymetric Compilation Group 2022: The GEBCO\_2022 Grid - a continuous terrain model of the global oceans and land., <https://doi.org/10.5285/E0F0BB80-AB44-2739-E053-6C86ABC0289C>, 2022.
- 530 Gonçalves-Araujo, R., Rabe, B., Peeken, I., and Bracher, A.: High colored dissolved organic matter (CDOM) absorption in surface waters of the central-eastern Arctic Ocean: Implications for biogeochemistry and ocean color algorithms, *PLoS ONE*, 13, e0190838, <https://doi.org/10.1371/journal.pone.0190838>, 2018.
- de Gouw, J. and Warneke, C.: Measurements of volatile organic compounds in the earth's atmosphere using proton-transfer-reaction mass spectrometry, *Mass Spectrom. Rev.*, 26, 223–257, <https://doi.org/10.1002/mas.20119>, 2007.
- 535 Gros, V., Bonsang, B., and Sarda Esteve, R.: Atmospheric carbon monoxide 'in situ' monitoring by automatic gas chromatography, *Chemosphere - Global Change Science*, 1, 153–161, [https://doi.org/10.1016/S1465-9972\(99\)00010-0](https://doi.org/10.1016/S1465-9972(99)00010-0), 1999.
- Gros, V., Peeken, I., Bluhm, K., Zöllner, E., Sarda-Esteve, R., and Bonsang, B.: Carbon monoxide emissions by phytoplankton: evidence from laboratory experiments, *Environ. Chem.*, 6, 369, <https://doi.org/10.1071/EN09020>, 2009.
- 540 Guenther, A., Hewitt, C. N., Erickson, D., Fall, R., Geron, C., Graedel, T., Harley, P., Klinger, L., Lerdau, M., McKay, W. A., Pierce, T., Scholes, B., Steinbrecher, R., Tallamraju, R., Taylor, J., and Zimmerman, P.: A global model of natural volatile organic compound emissions, *J. Geophys. Res.*, 100, 8873, <https://doi.org/10.1029/94JD02950>, 1995.
- Hackenberg, S. C., Andrews, S. J., Airs, R., Arnold, S. R., Bouman, H. A., Brewin, R. J. W., Chance, R. J., Cummings, D., Dall'Olmo, G., Lewis, A. C., Minaeian, J. K., Reifel, K. M., Small, A., Tarran, G. A., Tilstone, G. H., and Carpenter, L. J.: Potential controls of isoprene in the surface ocean: Isoprene Controls in the Surface Ocean, *Global Biogeochem. Cycles*, 31, 644–662, <https://doi.org/10.1002/2016GB005531>, 2017.
- 545 Hayashida, H., Carnat, G., Galí, M., Monahan, A. H., Mortenson, E., Sou, T., and Steiner, N. S.: Spatiotemporal Variability in Modeled Bottom Ice and Sea Surface Dimethylsulfide Concentrations and Fluxes in the Arctic During 1979–2015, *Global Biogeochem. Cycles*, 34, <https://doi.org/10.1029/2019GB006456>, 2020.

- 550 Hegseth, E. N. and Sundfjord, A.: Intrusion and blooming of Atlantic phytoplankton species in the high Arctic, *Journal of Marine Systems*, 74, 108–119, <https://doi.org/10.1016/j.jmarsys.2007.11.011>, 2008.
- Jackson, R. and Gabric, A.: Climate Change Impacts on the Marine Cycling of Biogenic Sulfur: A Review, *Microorganisms*, 10, 1581, <https://doi.org/10.3390/microorganisms10081581>, 2022.
- 555 Jacob, D. J., Field, B. D., Jin, E. M., Bey, I., Li, Q., Logan, J. A., Yantosca, R. M., and Singh, H. B.: Atmospheric budget of acetone: ATMOSPHERIC BUDGET OF ACETONE, *J. Geophys. Res.*, 107, ACH 5-1-ACH 5-17, <https://doi.org/10.1029/2001JD000694>, 2002.
- Jarníková, T., Dacey, J., Lizotte, M., Levasseur, M., and Tortell, P.: The distribution of methylated sulfur compounds, DMS and DMSP, in Canadian subarctic and Arctic marine waters during summer 2015, *Biogeosciences*, 15, 2449–2465, <https://doi.org/10.5194/bg-15-2449-2018>, 2018.
- 560 Kameyama, S., Tanimoto, H., Inomata, S., Tsunogai, U., Ooki, A., Takeda, S., Obata, H., Tsuda, A., and Uematsu, M.: High-resolution measurement of multiple volatile organic compounds dissolved in seawater using equilibrator inlet–proton transfer reaction-mass spectrometry (EI–PTR-MS), *Marine Chemistry*, 122, 59–73, <https://doi.org/10.1016/j.marchem.2010.08.003>, 2010.
- Kansal, A.: Sources and reactivity of NMHCs and VOCs in the atmosphere: A review, *Journal of Hazardous Materials*, 166, 17–26, <https://doi.org/10.1016/j.jhazmat.2008.11.048>, 2009.
- 565 Kettle, A. J., Rhee, T. S., von Hobe, M., Poulton, A., Aiken, J., and Andreae, M. O.: Assessing the flux of different volatile sulfur gases from the ocean to the atmosphere, *J. Geophys. Res.*, 106, 12193–12209, <https://doi.org/10.1029/2000JD900630>, 2001.
- Kiene, R. P.: Production of methanethiol from dimethylsulfoniopropionate in marine surface waters, *Marine Chemistry*, 54, 69–83, [https://doi.org/10.1016/0304-4203\(96\)00006-0](https://doi.org/10.1016/0304-4203(96)00006-0), 1996.
- 570 Kiene, R. P. and Linn, L. J.: The fate of dissolved dimethylsulfoniopropionate (DMSP) in seawater: tracer studies using <sup>35</sup>S-DMSP, *Geochimica et Cosmochimica Acta*, 64, 2797–2810, [https://doi.org/10.1016/S0016-7037\(00\)00399-9](https://doi.org/10.1016/S0016-7037(00)00399-9), 2000.
- Kiene, R. P., Williams T.E., Esson, K., Tortell, P., and Dacey, J.W. H.: Concentrations and Sea-Air Fluxes in the Subarctic NE Pacific Ocean, AGU, Fall Meeting, San Francisco, 2017.
- 575 Kilgour, D. B., Novak, G. A., Sauer, J. S., Moore, A. N., Dinasquet, J., Amiri, S., Franklin, E. B., Mayer, K., Winter, M., Morris, C. K., Price, T., Malfatti, F., Crocker, D. R., Lee, C., Cappa, C. D., Goldstein, A. H., Prather, K. A., and Bertram, T. H.: Marine gas-phase sulfur emissions during an induced phytoplankton bloom, *Atmos. Chem. Phys.*, 22, 1601–1613, <https://doi.org/10.5194/acp-22-1601-2022>, 2022.
- Kloster, S., Feichter, J., Maier-Reimer, E., Six, K. D., Stier, P., and Wetzell, P.: DMS cycle in the marine ocean-atmosphere system – a global model study, *Biogeosciences*, 3, 29–51, <https://doi.org/10.5194/bg-3-29-2006>, 2006.
- 580 Lana, A., Simó, R., Vallina, S. M., and Dachs, J.: Re-examination of global emerging patterns of ocean DMS concentration, *Biogeochemistry*, 110, 173–182, <https://doi.org/10.1007/s10533-011-9677-9>, 2012.
- Landa, M., Burns, A. S., Durham, B. P., Esson, K., Nowinski, B., Sharma, S., Vorobev, A., Nielsen, T., Kiene, R. P., and Moran, M. A.: Sulfur metabolites that facilitate oceanic phytoplankton–bacteria carbon flux, *ISME J*, 13, 2536–2550, <https://doi.org/10.1038/s41396-019-0455-3>, 2019.

- 585 Lannuzel, D., Tedesco, L., van Leeuwe, M., Campbell, K., Flores, H., Delille, B., Miller, L., Stefels, J., Assmy, P., Bowman, J., Brown, K., Castellani, G., Chierici, M., Crabeck, O., Damm, E., Else, B., Fransson, A., Fripiat, F., Geilfus, N.-X., Jacques, C., Jones, E., Kaartokallio, H., Kotovitch, M., Meiners, K., Moreau, S., Nomura, D., Peeken, I., Rintala, J.-M., Steiner, N., Tison, J.-L., Vancoppenolle, M., Van der Linden, F., Vichi, M., and Wongpan, P.: The future of Arctic sea-ice biogeochemistry and ice-associated ecosystems, *Nat. Clim. Chang.*, 10, 983–992, <https://doi.org/10.1038/s41558-020-00940-4>, 2020.
- 590 Lawson, S. J., Law, C. S., Harvey, M. J., Bell, T. G., Walker, C. F., de Bruyn, W. J., and Saltzman, E. S.: Methanethiol, dimethyl sulfide and acetone over biologically productive waters in the southwest Pacific Ocean, *Atmos. Chem. Phys.*, 20, 3061–3078, <https://doi.org/10.5194/acp-20-3061-2020>, 2020.
- Leck, C. and Rodhe, H.: Emissions of marine biogenic sulfur to the atmosphere of northern Europe, *J Atmos Chem*, 12, 63–86, <https://doi.org/10.1007/BF00053934>, 1991.
- 595 Levasseur, M.: Impact of Arctic meltdown on the microbial cycling of sulphur, *Nature Geosci*, 6, 691–700, <https://doi.org/10.1038/ngeo1910>, 2013.
- Lindinger, W. and Jordan, A.: Proton-transfer-reaction mass spectrometry (PTR–MS): on-line monitoring of volatile organic compounds at pptv levels, *Chem. Soc. Rev.*, 27, 347, <https://doi.org/10.1039/a827347z>, 1998.
- Liu, J., Liu, J., Zhang, S.-H., Liang, J., Lin, H., Song, D., Yang, G.-P., Todd, J. D., and Zhang, X.-H.: Novel Insights Into Bacterial Dimethylsulfoniopropionate Catabolism in the East China Sea, *Front. Microbiol.*, 9, 3206, <https://doi.org/10.3389/fmicb.2018.03206>, 2018.
- 600 Love, C. R., Arrington, E. C., Gosselin, K. M., Reddy, C. M., Van Mooy, B. A. S., Nelson, R. K., and Valentine, D. L.: Microbial production and consumption of hydrocarbons in the global ocean, *Nat Microbiol*, 6, 489–498, <https://doi.org/10.1038/s41564-020-00859-8>, 2021.
- 605 Marandino, C. A.: Oceanic uptake and the global atmospheric acetone budget, *Geophys. Res. Lett.*, 32, L15806, <https://doi.org/10.1029/2005GL023285>, 2005.
- Martin, M.: Cutadapt removes adapter sequences from high-throughput sequencing reads, *EMBnet j.*, 17, 10, <https://doi.org/10.14806/ej.17.1.200>, 2011.
- Massicotte, P., Peeken, I., Katlein, C., Flores, H., Huot, Y., Castellani, G., Arndt, S., Lange, B. A., Tremblay, J., and Babin, M.: Sensitivity of Phytoplankton Primary Production Estimates to Available Irradiance Under Heterogeneous Sea Ice Conditions, *J. Geophys. Res. Oceans*, 124, 5436–5450, <https://doi.org/10.1029/2019JC015007>, 2019.
- 610 Metfies, K., Schroeder, F., Hessel, J., Wollschläger, J., Micheller, S., Wolf, C., Kiliyas, E., Sprong, P., Neuhaus, S., Frickenhaus, S., and Petersen, W.: High-resolution monitoring of marine protists based on an observation strategy integrating automated on-board filtration and molecular analyses, *Ocean Sci.*, 12, 1237–1247, <https://doi.org/10.5194/os-12-1237-2016>, 2016.
- 615 Metfies, K., Hessel, J., Klenk, R., Petersen, W., Wiltshire, K. H., and Kraberg, A.: Uncovering the intricacies of microbial community dynamics at Helgoland Roads at the end of a spring bloom using automated sampling and 18S meta-barcoding, *PLoS ONE*, 15, e0233921, <https://doi.org/10.1371/journal.pone.0233921>, 2020.
- Moran, M. A. and Durham, B. P.: Sulfur metabolites in the pelagic ocean, *Nat Rev Microbiol*, 17, 665–678, <https://doi.org/10.1038/s41579-019-0250-1>, 2019.
- 620 Moran, M. A., Reisch, C. R., Kiene, R. P., and Whitman, W. B.: Genomic Insights into Bacterial DMSP Transformations, *Annu. Rev. Mar. Sci.*, 4, 523–542, <https://doi.org/10.1146/annurev-marine-120710-100827>, 2012.

- Morel, A. and Gentili, B.: A simple band ratio technique to quantify the colored dissolved and detrital organic material from ocean color remotely sensed data, *Remote Sensing of Environment*, 113, 998–1011, <https://doi.org/10.1016/j.rse.2009.01.008>, 2009.
- 625 Mungall, E. L., Croft, B., Lizotte, M., Thomas, J. L., Murphy, J. G., Lepasseeur, M., Martin, R. V., Wentzell, J. J. B., Liggio, J., and Abbatt, J. P. D.: Dimethyl sulfide in the summertime Arctic atmosphere: measurements and source sensitivity simulations, *Atmos. Chem. Phys.*, 16, 6665–6680, <https://doi.org/10.5194/acp-16-6665-2016>, 2016.
- Nikolopoulos, Anna, Janout, Markus A, Hölemann, Jens A, Juhls, Bennet, Korhonen, Meri, and Randelhoff, Achim: Physical oceanography measured on water bottle samples during POLARSTERN cruise PS92 (ARK-XXIX/1),  
630 <https://doi.org/10.1594/PANGAEA.861866>, 2016.
- Nöthig, E.-M., Bracher, A., Engel, A., Metfies, K., Niehoff, B., Peeken, I., Bauerfeind, E., Cherkasheva, A., Gäbler-Schwarz, S., Hardge, K., Kiliyas, E., Kraft, A., Mebrahtom Kidane, Y., Lalande, C., Piontek, J., Thomisch, K., and Wurst, M.: Summertime plankton ecology in Fram Strait—a compilation of long- and short-term observations, *Polar Research*, 34, 23349, <https://doi.org/10.3402/polar.v34.23349>, 2015.
- 635 Novak, G. A., Kilgour, D. B., Jernigan, C. M., Vermeuel, M. P., and Bertram, T. H.: Oceanic emissions of dimethyl sulfide and methanethiol and their contribution to sulfur dioxide production in the marine atmosphere, *Atmos. Chem. Phys.*, 22, 6309–6325, <https://doi.org/10.5194/acp-22-6309-2022>, 2022.
- Nowinski, B., Motard-Côté, J., Landa, M., Preston, C. M., Scholin, C. A., Birch, J. M., Kiene, R. P., and Moran, M. A.: Microdiversity and temporal dynamics of marine bacterial dimethylsulfoniopropionate genes, *Environ Microbiol*, 21, 1687–  
640 1701, <https://doi.org/10.1111/1462-2920.14560>, 2019.
- Ooki, A., Nomura, D., Nishino, S., Kikuchi, T., and Yokouchi, Y.: A global-scale map of isoprene and volatile organic iodine in surface seawater of the Arctic, Northwest Pacific, Indian, and Southern Oceans, *J. Geophys. Res. Oceans*, 120, 4108–4128, <https://doi.org/10.1002/2014JC010519>, 2015.
- Oziel, L., Baudena, A., Ardyna, M., Massicotte, P., Randelhoff, A., Sallée, J.-B., Ingvaldsen, R. B., Devred, E., and Babin, M.: Faster Atlantic currents drive poleward expansion of temperate phytoplankton in the Arctic Ocean, *Nat Commun*, 11, 1705, <https://doi.org/10.1038/s41467-020-15485-5>, 2020.
- Parada, A. E., Needham, D. M., and Fuhrman, J. A.: Every base matters: assessing small subunit rRNA primers for marine microbiomes with mock communities, time series and global field samples: Primers for marine microbiome studies, *Environ Microbiol*, 18, 1403–1414, <https://doi.org/10.1111/1462-2920.13023>, 2016.
- 650 Park, K.-T., Lee, K., Yoon, Y.-J., Lee, H.-W., Kim, H.-C., Lee, B.-Y., Hermansen, O., Kim, T.-W., and Holmén, K.: Linking atmospheric dimethyl sulfide and the Arctic Ocean spring bloom: ATMOSPHERIC DMS IN THE ARCTIC SPRING BLOOM, *Geophys. Res. Lett.*, 40, 155–160, <https://doi.org/10.1029/2012GL054560>, 2013.
- Peeken, I.: The Expedition PS92 of the Research Vessel Polarstern to the Arctic Ocean in 2015, Alfred-Wegener-Institut, Helmholtz-Zentrum für Polar- und Meeresforschung, [https://doi.org/10.2312/BZPM\\_0694\\_2016](https://doi.org/10.2312/BZPM_0694_2016), 2016.
- 655 Petersen, W.: FerryBox systems: State-of-the-art in Europe and future development, *Journal of Marine Systems*, 140, 4–12, <https://doi.org/10.1016/j.jmarsys.2014.07.003>, 2014.
- Phillips, D. P., Hopkins, F. E., Bell, T. G., Liss, P. S., Nightingale, P. D., Reeves, C. E., Wohl, C., and Yang, M.: Air–sea exchange of acetone, acetaldehyde, DMS and isoprene at a UK coastal site, *Atmos. Chem. Phys.*, 21, 10111–10132, <https://doi.org/10.5194/acp-21-10111-2021>, 2021.



- 660 Polyakov, I. V., Alkire, M. B., Bluhm, B. A., Brown, K. A., Carmack, E. C., Chierici, M., Danielson, S. L., Ellingsen, I., Ershova, E. A., Gårdfeldt, K., Ingvaldsen, R. B., Pnyushkov, A. V., Slagstad, D., and Wassmann, P.: Borealization of the Arctic Ocean in Response to Anomalous Advection From Sub-Arctic Seas, *Front. Mar. Sci.*, 7, 491, <https://doi.org/10.3389/fmars.2020.00491>, 2020.
- 665 Quast, C., Pruesse, E., Yilmaz, P., Gerken, J., Schweer, T., Yarza, P., Peplies, J., and Glöckner, F. O.: The SILVA ribosomal RNA gene database project: improved data processing and web-based tools, *Nucleic Acids Research*, 41, D590–D596, <https://doi.org/10.1093/nar/gks1219>, 2012.
- Rodríguez-Ros, P., Cortés, P., Robinson, C. M., Nunes, S., Hassler, C., Royer, S.-J., Estrada, M., Sala, M. M., and Simó, R.: Distribution and Drivers of Marine Isoprene Concentration across the Southern Ocean, *Atmosphere*, 11, 556, <https://doi.org/10.3390/atmos11060556>, 2020.
- 670 Schmale, J., Zieger, P., and Ekman, A. M. L.: Aerosols in current and future Arctic climate, *Nat. Clim. Chang.*, 11, 95–105, <https://doi.org/10.1038/s41558-020-00969-5>, 2021.
- Shaw, G. E.: Bio-controlled thermostasis involving the sulfur cycle, *Climatic Change*, 5, 297–303, <https://doi.org/10.1007/BF02423524>, 1983.
- 675 Shaw, S. L., Gantt, B., and Meskhidze, N.: Production and Emissions of Marine Isoprene and Monoterpenes: A Review, *Advances in Meteorology*, 2010, 1–24, <https://doi.org/10.1155/2010/408696>, 2010.
- Simó, R., Cortés-Greus, P., Rodríguez-Ros, P., and Masdeu-Navarro, M.: Substantial loss of isoprene in the surface ocean due to chemical and biological consumption, *Commun Earth Environ*, 3, 20, <https://doi.org/10.1038/s43247-022-00352-6>, 2022.
- Singh, H. B.: In situ measurements of HCN and CH<sub>3</sub>CN over the Pacific Ocean: Sources, sinks, and budgets, *J. Geophys. Res.*, 108, 8795, <https://doi.org/10.1029/2002JD003006>, 2003.
- 680 Singh, H. B.: Analysis of the atmospheric distribution, sources, and sinks of oxygenated volatile organic chemicals based on measurements over the Pacific during TRACE-P, *J. Geophys. Res.*, 109, D15S07, <https://doi.org/10.1029/2003JD003883>, 2004.
- 685 Song, G., Xie, H., Aubry, C., Zhang, Y., Gosselin, M., Mundy, C. J., Philippe, B., and Papakyriakou, T. N.: Spatiotemporal variations of dissolved organic carbon and carbon monoxide in first-year sea ice in the western Canadian Arctic, *J. Geophys. Res.*, 116, C00G05, <https://doi.org/10.1029/2010JC006867>, 2011.
- Stefels, J., Steinke, M., Turner, S., Malin, G., and Belviso, S.: Environmental constraints on the production and removal of the climatically active gas dimethylsulphide (DMS) and implications for ecosystem modelling, *Biogeochemistry*, 83, 245–275, <https://doi.org/10.1007/s10533-007-9091-5>, 2007.
- 690 Sun, J., Todd, J. D., Thrash, J. C., Qian, Y., Qian, M. C., Temperton, B., Guo, J., Fowler, E. K., Aldrich, J. T., Nicora, C. D., Lipton, M. S., Smith, R. D., De Leenheer, P., Payne, S. H., Johnston, A. W. B., Davie-Martin, C. L., Halsey, K. H., and Giovannoni, S. J.: The abundant marine bacterium *Pelagibacter* simultaneously catabolizes dimethylsulfoniopropionate to the gases dimethyl sulfide and methanethiol, *Nat Microbiol*, 1, 16065, <https://doi.org/10.1038/nmicrobiol.2016.65>, 2016.
- 695 Sunagawa, S., Coelho, L. P., Chaffron, S., Kultima, J. R., Labadie, K., Salazar, G., Djahanschiri, B., Zeller, G., Mende, D. R., Alberti, A., Cornejo-Castillo, F. M., Costea, P. I., Cruaud, C., d’Ovidio, F., Engelen, S., Ferrera, I., Gasol, J. M., Guidi, L., Hildebrand, F., Kokoszka, F., Lepoivre, C., Lima-Mendez, G., Poulain, J., Poulos, B. T., Royo-Llonch, M., Sarmiento, H., Vieira-Silva, S., Dimier, C., Picheral, M., Searson, S., Kandels-Lewis, S., Tara Oceans coordinators, Bowler, C., de Vargas, C., Gorsky, G., Grimsley, N., Hingamp, P., Iudicone, D., Jaillon, O., Not, F., Ogata, H., Pesant, S., Speich, S., Stemmann, L.,

- 700 Sullivan, M. B., Weissenbach, J., Wincker, P., Karsenti, E., Raes, J., Acinas, S. G., Bork, P., Boss, E., Bowler, C., Follows, M., Karp-Boss, L., Krzic, U., Reynaud, E. G., Sardet, C., Sieracki, M., and Velayoudon, D.: Structure and function of the global ocean microbiome, *Science*, 348, 1261359, <https://doi.org/10.1126/science.1261359>, 2015.
- Tanimoto, H., Kameyama, S., Omori, Y., Inomata, S., and Tsunogai, U.: High-Resolution Measurement of Volatile Organic Compounds Dissolved in Seawater Using Equilibrator Inlet-Proton Transfer Reaction-Mass Spectrometry (EI-PTR-MS), in: *Western Pacific Air-Sea Interaction Study*, edited by: Uematsu, M., Yokouchi, Y., Watanabe, Y., Takeda, S., and Yamanaka, Y., TERRAPUB, 89–115, <https://doi.org/10.5047/w-pass.a02.001>, 2014.
- 705 Thompson, H. F., Summers, S., Yucel, R., and Gutierrez, T.: Hydrocarbon-Degrading Bacteria Found Tightly Associated with the 50–70  $\mu\text{m}$  Cell-Size Population of Eukaryotic Phytoplankton in Surface Waters of a Northeast Atlantic Region, *Microorganisms*, 8, 1955, <https://doi.org/10.3390/microorganisms8121955>, 2020.
- 710 Tison, J.-L., Brabant, F., Dumont, I., and Stefels, J.: High-resolution dimethyl sulfide and dimethylsulfoniopropionate time series profiles in decaying summer first-year sea ice at Ice Station Polarstern, western Weddell Sea, Antarctica, *J. Geophys. Res.*, 115, G04044, <https://doi.org/10.1029/2010JG001427>, 2010.
- Tolli, J. D. and Taylor, C. D.: Biological CO oxidation in the Sargasso Sea and in Vineyard Sound, Massachusetts, *Limnol. Oceanogr.*, 50, 1205–1212, <https://doi.org/10.4319/lo.2005.50.4.1205>, 2005.
- 715 Tran, S., Bonsang, B., Gros, V., Peeken, I., Sarda-Esteve, R., Bernhardt, A., and Belviso, S.: A survey of carbon monoxide and non-methane hydrocarbons in the Arctic Ocean during summer 2010, *Biogeosciences*, 10, 1909–1935, <https://doi.org/10.5194/bg-10-1909-2013>, 2013.
- Tyndall, G. S. and Ravishankara, A. R.: Atmospheric oxidation of reduced sulfur species, *Int. J. Chem. Kinet.*, 23, 483–527, <https://doi.org/10.1002/kin.550230604>, 1991.
- 720 Uhlig, C., Damm, E., Peeken, I., Krumpfen, T., Rabe, B., Korhonen, M., and Ludwighowski, K.-U.: Sea Ice and Water Mass Influence Dimethylsulfide Concentrations in the Central Arctic Ocean, *Front. Earth Sci.*, 7, 179, <https://doi.org/10.3389/feart.2019.00179>, 2019.
- Vila-Costa, M., Simó, R., Harada, H., Gasol, J. M., Slezak, D., and Kiene, R. P.: Dimethylsulfoniopropionate Uptake by Marine Phytoplankton, *Science*, 314, 652–654, <https://doi.org/10.1126/science.1131043>, 2006.
- 725 Wang, S., Hornbrook, R. S., Hills, A., Emmons, L. K., Tilmes, S., Lamarque, J., Jimenez, J. L., Campuzano-Jost, P., Nault, B. A., Crouse, J. D., Wennberg, P. O., Kim, M., Allen, H., Ryerson, T. B., Thompson, C. R., Peischl, J., Moore, F., Nance, D., Hall, B., Elkins, J., Tanner, D., Huey, L. G., Hall, S. R., Ullmann, K., Orlando, J. J., Tyndall, G. S., Flocke, F. M., Ray, E., Hanisco, T. F., Wolfe, G. M., St. Clair, J., Commane, R., Daube, B., Barletta, B., Blake, D. R., Weinzierl, B., Dollner, M., Conley, A., Vitt, F., Wofsy, S. C., Riemer, D. D., and Apel, E. C.: Atmospheric Acetaldehyde: Importance of Air-Sea Exchange and a Missing Source in the Remote Troposphere, *Geophys. Res. Lett.*, 46, 5601–5613, <https://doi.org/10.1029/2019GL082034>, 2019.
- 730 Williams, J., Holzinger, R., Gros, V., Xu, X., Atlas, E., and Wallace, D. W. R.: Measurements of organic species in air and seawater from the tropical Atlantic: ORGANIC SPECIES IN AIR AND SEA, *Geophys. Res. Lett.*, 31, <https://doi.org/10.1029/2004GL020012>, 2004.
- 735 Wilson, D. F., Swinnerton, J. W., and Lamontagne, R. A.: Production of Carbon Monoxide and Gaseous Hydrocarbons in Seawater: Relation to Dissolved Organic Carbon, *Science*, 168, 1577–1579, <https://doi.org/10.1126/science.168.3939.1577>, 1970.

- Wohl, C., Capelle, D., Jones, A., Sturges, W. T., Nightingale, P. D., Else, B. G. T., and Yang, M.: Segmented flow coil equilibrator coupled to a proton-transfer-reaction mass spectrometer for measurements of a broad range of volatile organic compounds in seawater, *Ocean Sci.*, 15, 925–940, <https://doi.org/10.5194/os-15-925-2019>, 2019.
- 740 Wohl, C., Brown, I., Kitidis, V., Jones, A. E., Sturges, W. T., Nightingale, P. D., and Yang, M.: Underway seawater and atmospheric measurements of volatile organic compounds in the Southern Ocean, *Biogeosciences*, 17, 2593–2619, <https://doi.org/10.5194/bg-17-2593-2020>, 2020.
- Wohl, C., Jones, A. E., Sturges, W. T., Nightingale, P. D., Else, B., Butterworth, B. J., and Yang, M.: Sea ice concentration impacts dissolved organic gases in the Canadian Arctic, *Biogeosciences*, 19, 1021–1045, <https://doi.org/10.5194/bg-19-1021-2022>, 2022.
- 745 Wollenburg, J. E., Katlein, C., Nehrke, G., Nöthig, E.-M., Matthiessen, J., Wolf-Gladrow, D. A., Nikolopoulos, A., Gázquez-Sánchez, F., Rossmann, L., Assmy, P., Babin, M., Bruyant, F., Beaulieu, M., Dybwad, C., and Peeken, I.: Ballasting by cryogenic gypsum enhances carbon export in a *Phaeocystis* under-ice bloom, *Sci Rep*, 8, 7703, <https://doi.org/10.1038/s41598-018-26016-0>, 2018.
- 750 Xie, H. and Gosselin, M.: Photoproduction of carbon monoxide in first-year sea ice in Franklin Bay, southeastern Beaufort Sea: PHOTOPRODUCTION OF CO IN SEA ICE, *Geophys. Res. Lett.*, 32, n/a-n/a, <https://doi.org/10.1029/2005GL022803>, 2005.
- Xie, H. and Zafiriou, O. C.: Evidence for significant photochemical production of carbon monoxide by particles in coastal and oligotrophic marine waters, *Geophys. Res. Lett.*, 36, L23606, <https://doi.org/10.1029/2009GL041158>, 2009.
- 755 Yang, M., Beale, R., Liss, P., Johnson, M., Blomquist, B., and Nightingale, P.: Air–sea fluxes of oxygenated volatile organic compounds across the Atlantic Ocean, *Atmos. Chem. Phys.*, 14, 7499–7517, <https://doi.org/10.5194/acp-14-7499-2014>, 2014.
- Yuan, B., Koss, A. R., Warneke, C., Coggon, M., Sekimoto, K., and de Gouw, J. A.: Proton-Transfer-Reaction Mass Spectrometry: Applications in Atmospheric Sciences, *Chem. Rev.*, 117, 13187–13229, <https://doi.org/10.1021/acs.chemrev.7b00325>, 2017.
- 760 Zannoni, N., Gros, V., Lanza, M., Sarda, R., Bonsang, B., Kalogridis, C., Preunkert, S., Legrand, M., Jambert, C., Boissard, C., and Lathiere, J.: OH reactivity and concentrations of biogenic volatile organic compounds in a Mediterranean forest of downy oak trees, *Atmos. Chem. Phys.*, 16, 1619–1636, <https://doi.org/10.5194/acp-16-1619-2016>, 2016.
- Zhou, X. and Mopper, K.: Photochemical production of low-molecular-weight carbonyl compounds in seawater and surface microlayer and their air-sea exchange, *Marine Chemistry*, 56, 201–213, [https://doi.org/10.1016/S0304-4203\(96\)00076-X](https://doi.org/10.1016/S0304-4203(96)00076-X), 1997.
- 765 Zhu, Y. and Kieber, D. J.: Concentrations and Photochemistry of Acetaldehyde, Glyoxal, and Methylglyoxal in the Northwest Atlantic Ocean, *Environ. Sci. Technol.*, 53, 9512–9521, <https://doi.org/10.1021/acs.est.9b01631>, 2019.

770

### **Author contributions**

VG, RSE, BB, and IP designed the study. BB, VG and RSE performed trace gas measurements prior to the campaign; VG and RSE performed trace gas measurements on-board. IP coordinated all TRANSSIZ work, and supervised the biological sampling onboard as well as subsequent performed pigment analyses. AN coordinated the oceanographic sampling and water mass classification. KM set up the AUTOFIM sampling system and supervised DNA extraction. MW performed bacterial community analyses. VG, BB, IP and MW wrote the manuscript. All co-authors have read and contributed to the manuscript.

775

### **Competing interests**

The authors declare no competing interests.

780

### **Acknowledgments**

We are thankful to the captain, crew and scientists from the TRANSSIZ expedition (ARK XXIX/1; PS92), carried out under grant number AWI\_PS92\_00. We thank Francois Truong for help with data processing, as well as Josephine Rapp and Halina Tegetmeyer for help with amplicon sequencing. We would like to thank the 3 anonymous reviewers who provided very useful comments that helped to improve the paper. IP, MW and KM are funded by the PoF IV program “Changing Earth - Sustaining our Future” Topic 6.1 of the Helmholtz Association. The publication is part of the FRAM Observatory under EPIC number 56216. We acknowledge financial support from AWI, CNRS and CEA.

785